X-612-66-381

NASA TM X- 55605

OBSERVATIONS OF THE SOLAR WIND INTERACTION WITH THE GEOMAGNETIC FIELD: CONDITIONS QUIET

BY

NORMAN F. NESS

AUGUST 1966

GODDARD SPACE FLIGHT CENTER

GREENBELT, MARYLAND

OBSERVATIONS OF THE SOLAR WIND INTERACTION WITH THE GEOMAGNETIC FIELD: CONDITIONS QUIET

Norman F. Ness
Laboratory for Space Sciences
Goddard Space Flight Center
Greenbelt, Maryland USA

August 1966

Introduction

Until relatively recently the sun was thought to be a source of ionized gaseous and energetic particle emissions for only short periods of time following the development of solar flares. These temporary emissions propagated into interplanetary space and subsequently interacted with the atmosphere and magnetic field of the earth to produce significant fluctuations in various geophysical parameters. Most characteristic were the magnetic storm and associated auroral phenomena which lead Chapman and Ferraro and subsequent workers to investigate the possibility of confining the geomagnetic field within a finite volume by the expanding solar plasma. Since this paper is not concerned with the discussion of transient disturbances but only the steady state we shall not include a discussion of this earlier work or the most recent satellite measurements on the magnetic storm phenomena.

The investigation of magnetic storms led Chapman and subsequently Chamberlain and Parker to study in more detail the state of the atmosphere of the sun and its extension into interplanetary space. This work was stimulated by Biermann's study of type I ionized gas comet tails. Thus, in 1957 when the exploration of space by artificial earth satellites was begun, the concept of the physical properties of interplanetary space were undergoing a major revision. Theoretical work, principally by Parker, suggested a continual flux of substantial plasma from the sun because of the very high temperatures on its surface. Direct measurements by satellites have confirmed the existence of a continuous solar plasma, the solar wind, and have provided detailed measurements of its interaction with the geomagnetic field. This paper is concerned with reviewing those experiments which provide information on the steady state of the outer geomagnetic field and the solar wind interaction with it. We shall begin with a brief historical review of the first five years (1957-1962) experiments and their interpretation. We shall then discuss the most recent results obtained since 1963 with essentially "second generation" satellite experiments which have provided increasingly more detailed and definitive measurements as well as discovering important new aspects of these phenomena.

A chronological summary of those spacecraft which have provided measurements of the magnetic fields in space is presented in Table 1. Their pertinent spacecraft orbital characteristics and experiment parameters are also included. Certain of the spacecraft, as indicated with an asterisk, have also included plasma detectors sensitive to either electrons or ions with energies less than 10 kev. These essentially are most important in the investigation of the solar wind interaction with the geomagnetic field. This paper will discuss mainly magnetic field and plasma results as well as certain energetic particle measurements which are appropriate to this paper. The general problem of energetic particles in the magnetosphere is covered in another review paper of this meeting.

As a result of the flux of low energy plasma from the Sun and the effects of its interaction with the geomagnetic field, extraterrestrial space is now considered to be divided into three regions:

(i) The interplanetary region where the properties of the interplanetary medium are undisturbed by the presence of the Earth, and its magnetic field.

(ii) The magnetosheath , associated with the interaction of the solar wind with the geomagnetic field.

(iii) The magnetosphere, that region of space containing the geomagnetic field (the classical Chapman-Ferraro geomagnetic cavity.)

Separating these three regions of space are two surfaces whose physical characteristics have only recently been investigated:

(i) The collisionless magnetohydrodynamic shock wave surface separating the undisturbed interplanetary medium from the magnetosheath.

(ii) The magnetopause, separating the interaction region from the magnetosphere.

Historical Review

The first measurements of the outer region of the magnetosphere were made in 1958 on the Pioneer I space probe by Sonett (1960) and co-workers, Sonett et al.(1960a, c). Measurements of the field magnitude perpendicular to the spin axis of the spacecraft were performed with a search coil magnetometer. Data transmission was discontinuous and covered only the geocentric distance range 3.7-7 R_e and 12.3-14.8 R_e (earth radii) on the sunward side of the earth (see Figure 1). The data obtained closest to the earth indicated that the geomagnetic field was approximately dipolar. The second transmission indicated an abrupt decrease of field magnitude and a substantial increase in rapid fluctuations. The original analysis and interpretation of this data proposed an unmeasured but inferred traversal of the boundary of the geomagnetic field near 14 R_e due to the flux of the as yet undetected solar wind.

In 1959 Lunik I and II measurements of the geomagnetic field close to the earth detected large depressions of the main field between 2.8-4 R_e (Dolginov et al., 1960; 1961a, b). These results were interpreted to be indicative of the classical ring current associated with magnetic storm main phase disturbances. At approximately the same time, detailed mapping of the geomagnetic field between 2-7.5 R_e was performed by the Explorer 6 satellite (Smith et al., 1960; Sonett et al., 1960b). These measurements again yielded only the magnitude of the field perpendicular to the spin axis of the satellite but did include a phase angle measurement relative to the satellite-sun line. The large decrease in magnetic field noted at large distances from the earth were initially interpreted to represent the magnetic effects of a large scale permanent ring current at a distance of 10 R_e. The results of the Vanguard III proton magnetometer total field measurements in 1959 (Cain et al., 1962) were limited to less than 1.5 R_e and showed that any permanent ring current which existed must be above several R_e.

The Pioneer 5 satellite, which went into solar orbit, crossed the outer region of the geomagnetic field in 1960 and provided discontinuous measurements between 5-30 R_e (Coleman et al., 1960b, Coleman 1964). Results from this experiment, again measuring only the component of the magnetic field perpendicular to the spin axis showed an approximately dipolar decrease of the field from 5-9 R_e. Discontinuous transmission again precluded obtaining data during the traversal of the geomagnetic field boundary. The interplanetary magnetic field measurements by Pioneer 5, however, contributed importantly to subsequent theoretical studies of the solar wind interaction with the geomagnetic field. The results of Pioneer 5 were interpreted initially to indicate an interplanetary magnetic field mainly perpendicular to the ecliptic plane (Coleman et al., 1960a). In studying these results, Dungey (1961) suggested that there would be two characteristically different configurations to the geomagnetic field as a result of the possible interconnection of interplanetary and geomagnetic field lines.

The first observations of the magnetospheric boundary were performed by Explorer 10 in March 1961 with experiments measuring the vector magnetic field and low energy positively charged portion of the solar plasma. Since the orbit was oriented away from the sun as shown in Figure 1, the satellite never penetrated into the interplanetary medium but actually paralleled the magnetosphere boundary. The early publications by Bridge et al., (1962), and Heppner et al., (1962) indicated the preliminary understanding of the solar wind interaction with the geomagnetic field. It was a short while before the separate data were analyzed in a complimentary fashion (Heppner et al., 1963 and Bonneti et al., 1963). These interpretations were based upon the suggestions by Axford (1960), Kellogg (1962), and Rossi (1963) that a detached bow shock wave encompassing the distorted geomagnetic field would develop due to the supersonic flow of the solar wind. The plasma measurements on this satellite were the first to yield information on the composition and spectral characteristics in the magnetosheath (Scherb, 1964). Also the measurement of a highly distorted geomagnetic field due to the solar wind interaction led to a re-examination of the earlier Explorer 6 ring current results (Smith, 1962; Smith et al., 1964). These studies showed that the separate satellite results were consistent only in the context of an extended geomagnetic field on the night side of the earth and not a ring current as previously supposed.

The intimate relationship of fields and plasma at the magnetopause were established by Explorer 10. In an interval of 48 hours, the magnetosphere boundary was observed to move back and forth many times across the orbit of the satellite. The magnetospheric field was observed to be much stronger than predicted by extrapolation of the geomagnetic field at these large radial distances, 20-40 R_e. In addition positive correlation between the absence of plasma and the presence of a strong stable magnetic field representing the distortion of the geomagnetic field were clearly evident. When plasma was observed, the magnetic field tended to be weaker and to fluctuate much more rapidly. Explorer 10 thus established the presence of the boundary of the geomagnetic field as well as detecting motion of the boundary. However, the cause of the motion is not yet understood. Three possibilities suggest an explanation:

1. Waves on the surface of the magnetosphere boundary,
2. The expansion and contraction of the entire magnetosphere in response to varying solar wind flux, or finally,
3. A change in the relative position or "aspect" of the boundary due to the varying angle between the earth's magnetic dipole axis and the solar wind flow velocity.

The first measurements of trapped particles, fields and plasmas at the boundary of the geomagnetic field were conducted late in 1961 by the Explorer 14 satellite (Cahill and Amazeen, 1963; Freeman et al., 1963). These data, shown in Figure 2, indicate clearly a termination of the regular geomagnetic field compressed by the solar wind flow at a subsolar distance of approximately 8.2 R_e. This was coincident with the termination of the trapping of the energetic particles as well as the appearance of a low energy plasma presumed to represent the thermalized solar plasma.

These measurements from Explorers 10 and 12 demonstrated that there was a permanent existance of the confined geomagnetic field. With the direct measurements of the boundaries of the geomagnetic field it was also possible to place in proper perspective the earlier exploratory measurements by the Pioneers 1 and 5 and Explorer 6 satellites. Contemporary reviews of these early data have been provided by Obayashi (1964) and Cahill (1964b).

The detailed electron measurements performed on the relatively long lived Explorer 12 satellite by Freeman (1964) showed in addition to a termination of the regular geomagnetic field, the apparent termination of the quasi-thermalized plasma (see Figure 3). This was interpreted to reflect the presence of the collisionless bow shock wave predicted in the work previously referenced.

Thus, it was possible with the results from Explorer 10 and 12 published during 1962 and 1963 to consider the geometry of the earth's magnetic field distorted by the solar wind as given in Figure 4. The position of the geomagnetic cavity boundary is shown as detected by the early results from Explorer 12. There is an indication also of the inner and outer radiation belts as they were then known. This figure should be compared with the last figure of this paper for an indication of the rapid advance in our understanding of the geomagnetic field geometry in the last three years of space investigations.

Magnetosphere Boundary and Shock Wave Observations Since 1963

A comprehensive survey of the geomagnetic field boundary and the first magnetic measurements of the collisionless shock wave were performed by the IMP-I satellite in late 1963 (Ness et al., 1964, 1965) (see Figure 5). A sample of the results obtained is shown in Figure 6 from orbit number 1 corresponding to a traversal of the magnetosphere boundary at a local time of approximately 1000. The magnitude of the field is observed to be larger than that predicted (shown as dashed) as the magnetosphere boundary is reached at 11.3 R_e. A fluctuating and weaker magnetic field is observed beyond until the shock wave is detected at a radial distance of 16.8 R_e. The figure indicates clearly the identifiable positions of these boundaries. The results are presented in solar ecliptic coordinates in which the latitude (θ) and longitude (ϕ) of the magnetic field vector are given relative to the ecliptic plane and the earth-sun line. In addition, an important feature of these data is that the rms deviation of the magnetic field fluctuations over the time interval of 5.46 minutes are included. This provides a measure of the high frequency component of magnetic field fluctuations and has proven to be particularly diagnostic in the identification of the position of the collisionless shock wave since large rapid magnetic fluctuations are found to be characteristic of the magnetosheath region.

This characteristic behavior of the magnetic field, suggested earlier by Explorers 12 and 14, was repeated over 40 times while the IMP-I satellite apogee precessed from close to the subsolar region to the midnight meridian plane. In addition to the conspicious features observed as indicative of the magnetosphere boundary from the magnetic field measurements, the corresponding plasma results obtained by Bridge et al., (1965) and Wolfe et al., (1966a) confirmed the positional identification of abrupt changes in properties of the plasma. The early interpretation of the work by the MIT group (Bridge et al., 1965) suggested the presence of an almost isotropic thermalized plasma flow behind the shock near the subsolar point within the magnetosheath. The correspondence of the appearance of the isotropic thermalized flux was very good considering the separate identification made by the independent workers. However, the work by Wolfe et al., (1966a) on the same satellite indicated that while the plasma was disordered at the shock(and whose positions were in general agreement with the magnetic field measurements) they disagreed in the degree of isotropy of directional flow. Most recently Olbert (1966, private communication) has indicated that the presence of a large flux of low energy electrons (below 100 ev) were significant contributors to the results of the measurements in this region of space and a complete re-examination of these data is currently underway. The important point here is that the presence of a turbulent plasma as reflected in the spectrum in the magnetosheath corresponds uniquely well with the magnetic field data which detected a rapidly fluctuating magnetic field stronger than the interplanetary field.

Also on board the IMP-I satellite were energetic particle detectors sensitive to more energetic particles characteristic of the radiation belts. The result of Anderson et al., (1965) is represented in Figure 7 showing the characteristics of the particle flux observed on a traversal of the magnetosphere by the IMP-I satellite. The relative position of the magnetosphere boundary and shock as determined by the magnetic field measurements is shown for reference. The presence of intense transient fluxes of electrons with energy greater than 45 kev is a characteristic feature of these results. Anderson et al., (1965) has referred to these particle events as electron spikes and have attempted to utilize them in defining the extent of the magnetosheath and shock wave. Fan et al., (1964) initially attempted to interpret the position of the spikes as occuring simultaneous with the shock wave. It is now known (Fan et al., 1966) that this is not true in general and that the electron events occur close to the shock but also within the magnetosheath as well as beyond the shock wave. Jokipii and Davis (1964) have attempted to interpret these spikes in terms of a particle acceleration mechanism acting at and near the shock wave. Jokipii (1966) has studied the propagation of these pulses and their spectral changes in the magnetosheath as the plasma flows around the geomagnetic field.

A summary of the positions of the boundaries as determined by the IMP-I satellite has been compared with the theoretical studies by Spreiter and Jones (1963) in Figure 8. The theoretical position of the boundaries of the magnetic field were determined on the basis of specular reflection of a plasma from the geomagnetic field in the solution of a boundary value problem in which the boundary conditions are known but the position of the boundary is unknown. Utilization of classical high-speed aerodynamics predicts the shape of the shock wave as shown.

There is at present disagreement as to whether or not a classical shock wave will develop standing off from the magnetosphere. Detailed studies of the mechanisms leading to the development of a collisionless shock wave with specific application to the solar wind interaction with the geomagnetic field are being conducted by a number of workers (Corday, 1965; Nordlinger, 1964). Although the details are not theoretically well understood, the observational evidence appears to indicate the presence of a shock-like phenomena. However, Bernstein et al. (1964), Fredericks et al. (1965), and Scarf et al (1965) contend that only a broad disordered region is present. These authors interpret the entire magnetosheath as a transition between interplanetary space and the magnetosphere. As will be evident in the subsequent data presentation, more recent satellite measurements still confirm the concept of a shock wave standing off from the magnetosphere.

Subsequent measurements on the IMP-II satellite have been analyzed with the added insight from the previously obtained IMP-I measurements. Characteristic results obtained by IMP-II for two orbits in late 1964 are shown in Figure 9. Clearly evident is the detection of the magnetosheath and shock wave as well as multiple shock wave crossings on orbit 22. The positions of the shock wave and its characteristics are in generally good agreement with those obtained with IMP-I. In addition to the magnetic field data there is included a measure of electron flux by Serbu and Maier (1966) providing an estimate of the isotropic flux of electrons with energy greater than approximately 5 electron volts. It is seen that the retarding potential analyzer indicates the presence of a large electron flux generally coincident with the magnetosheath. Note that when a multiple crossing of the shock wave boundary is observed (evident in the lower half of the figure at SW 2 and 3) the magnetosheath plasma also is observed to be present again. It should be noted, however, that at times, the nature of the boundary between the magnetosheath and the magnetosphere is rather diffuse and the structure of the magnetosheath does not appear well developed, as evidenced by the electron flux measurements. A sample of this is shown in orbit 8 on the out-bound pass. Although the shock is well developed the magnetosphere boundary in this particular orbit is not clearly identified (Fairfield et al., 1966).

On the same satellite measurements of the plasma spectrum by Wolfe et al., (1966b) have been compared with those obtained on OGO-I and Vela-2. These results are presented in Figure 10 showing the broad spectral distribution of the low energy plasma forming the turbulent solar wind in the magnetosheath. The relative shape of the spectra are quite similar suggesting little change of the characteristics of the plasma spectrum as it flows around the magnetosphere.

Measurements of the magnetic field near the shock wave boundary performed on the OGO-I satellite by both fluxgate and search coil magnetometers is presented in Figures 11 and 12. Although the OGO-I satellite was originally planned to be attitude stabilized a malfunction of the aspect system led to a spin-stabilized spacecraft. Thus, results obtained from directional detectors reflect the spin modulation of approximately 12 seconds period. Measurements of the magnetic field with a triaxial fluxgate magnetometer were obtained by Heppner (1965) and with the high data rates revealed detailed features of the shock wave previously undetected by earlier experiments. A sample of the data and the detection of quasi-sinusoidal wave forms and fluctuations at high frequency are shown in Figure 11. It is important to note that the large scale 12-second period fluctuations represent the spin modulation due to the rotating spacecraft. Note the occurrence of small amplitude fluctuations of approximately a few gammas near the shock wave boundary. Note also the increase in magnetic field as reflected in the peak-to-peak amplitude of the spin modulation.

Accompanying these data is the work of Holzer et al., (1966) reporting results measuring higher frequency fluctuations of the magnetic field with a triaxial search coil magnetometer on the same OGO-I satellite. Detailed measurements of the field fluctuations near the shock wave are shown in Figure 12. The lowest three channels are the wave form outputs of the three mutually orthogonal sensors. The Z (10) channel is the detected output of a band pass filter centered at 10 cps. The spin axis channel is a linear combination of the X, Y, and Z channels which represents the mathematical construction of the expected output of a sensor parallel to the spin axis. Two boundary crossings are observed as the satellite is out-bound from the earth indicating that the shock wave has moved past the slowly moving ($\sim$ 1 km/sec) satellite. It is not uniquely possible to determine the velocity of motion of the shock wave from a single satellite measurement of multiple boundary crossings. In some instances, the search coil experiment has shown the presence of 37 traversals of the shock wave in 18 hours on a single pass through the magnetosheath region. Again as detected on the Explorer 12 and IMP-I satellites, high frequency noise is present in the magnetic field in the magnetosheath which decreases abruptly at what is interpreted to represent the shock wave. The positions of the shock wave and magnetosphere boundary as determined from these two experiments is generally in good agreement with those obtained previously.

The recent results obtained from the Pioneer 6 satellite near the sunset terminator are shown in Figure 13. Traversal of both the magnetopause and shock wave are shown indicating again the existance of relatively weak but rapidly fluctuating magnetic fields in the magnetosheath abruptly terminated at the shock wave but not quite so abruptly at the magnetopause. In this case a single observation of the boundary has been made. Note the presence of long period (approximately five minutes) fluctuations of the magnetic field interior to the magnetosphere boundary. Detailed analysis reveals the presence of MHD waves within the magnetosphere. Similar low frequency waves have also been observed on the Mariner IV satellite (Siscoe et al., 1966) which traversed the magnetopause near the sunrise terminator (see Figure 5).

The most comprehensive survey of the positions of the magnetopause and shock wave with one satellite have been performed with IMP-3. These measurements, obtained in 1965, are presented in Figure 14 in the same coordinate system used previously to analyze the IMP-1 boundary positions. The results obtained on the dawn side of the earth from IMP-1 and IMP-3 are in general agreement with each other and with previous measurements performed by Explorers 12 and 14 in this region of space. The important feature of these IMP-3 measurements is the extension of the boundary positions corresponding to the dusk side of the earth. Note that the positions are not symmetrically located about the earth-sun line but rather that they reflect the anticipated aberration effect of the earth's motion through the interplanetary medium.

In the interpretation of boundary positions it is important to take into account the varying angle of attack which the geomagnetic dipole presents to the solar plasma flow. This leads to an expansion and change in size of the magnetosphere and the corresponding position of the shock and magnetosphere as the geomagnetic latitude of the solar point changes periodically. In concluding this section, satellite experiments have established the existence of the magnetosphere boundary as a definitive separation of strong and stable magnetic fields of geomagnetic origin within the magnetosphere and rapidly fluctuating weaker magnetic fields of interplanetary origin in the magnetosheath.

The magnetosheath contains a thermalized solar plasma of low energy which develops at what many investigators consider to be a collisionless MHD shock wave. The detailed aspects of the magnetic field reveal wave-like fluctuations at the shock as well as within the magnetosphere. Since certain of the data contained in this review are the results of preliminary investigations it can be anticipated that substantial improvement in the understanding of the field and plasma results will be obtained when complete analysis of the OGO-1 and IMP-2 data are completed and published. Motion of the boundaries has been detected on many satellites even in the absence of any solar activity.

The magnetosphere boundary on the sunlit side appears to be roughly spherical in shape with a radius of curvature of 14 R_e centered 3.5 R_e behind the earth along the earth-sun line (Ness, 1965). The shock wave is observed to be roughly parabolic with an intercept of the earth-sun line at 14 R_e. Both boundaries are frequently in motion and have been detected as much as 20% from these nominal quoted values.

Geomagnetic Tail and Neutral Sheet

The measurements of the earth's magnetic field at great distances were begun by Explorer 10 in 1961. These results indicated the distortion of the geomagnetic field on the night side of the earth in which lines of force were observed to trail out far behind the earth and pointing roughly away from it. Subsequently in 1962 Explorer 14 (Cahill, 1964a; 1966) revealed near midnight local time, a distortion of the terrestial field so as to approach predominately an anti-solar direction out to distances of 16 R_e. The character of the magnetic field on the night side of the earth previously illustrated in Figure 4 was modified and theoretical suggestions made by Dessler and Axford et al. as shown in Figure 15. Such a tail-like appendage to the geomagnetic field was also suggested in the work of Piddington (1960) on the basis of a model for magnetic storms.

Detailed measurements mapping the earth's magnetic tail and discovery of the imbedded neutral sheet were performed in 1965 by the IMP-1 satellite (Ness, 1965). These data showed that the geomagnetic field extends out far behind the earth at least half way to the moon. The work of Axford et al., (1965), Dessler (1964) and Dessler and Juday (1965), present discussions of the configuration to be expected as the solar wind extends the geomagnetic field from the polar cap regions behind it to form the comet-like magnetic tail. Fluxgate magnetometer data from orbit number 41 of the IMP-1 satellite are presented in Figure 16 for that orbit closest to the midnight meridian plane. The results are presented in the solar ecliptic coordinate system and demonstrate the remarkable feature that t... magnetic field is oriented parallel to the earth-sun line ($\theta = 0^o$, $\phi = 0^o$, 180^o) with sense either towards ($\phi = 0^o$) or away ($\phi = 180^o$) from the sun depending upon whether or not the satellite is above or below a magnetically neutral surface identified as a neutral sheet.

The work of Axford et al. (1965) (see Figure 15) pointed out the existence of enhanced plasma fluxes in the neutral sheet region. This was suggested by the Explorer 14 results in 1962 (Frank, 1965; Frank and Van Allen, 1964) in which an energetic particle tail to the radiation belts was interpreted to exist on the night side of the earth. More recently measurements on the Vela satellites by Bame et al. (1966) have discussed the existence of a plasma sheet which is generally assumed to be coincident with the magnetic neutral sheet although simultaneous magnetic field measurements are not available.

The magnetic neutral sheet is observed to be an extremely thin feature, on the scale of a fraction of an earth radius. However, it is impossible on any one satellite traversal to determine uniquely the thickness without a priori assumptions as to the invariance of the position, orientation and thickness of the sheet during a single satellite traversal. It also depends upon the model of the field reversal which is employed as to what the effective "thickness" of the sheet may be. Indeed the limited spatial coverage by a particular satellite may limit the apparent thickness of the sheet as determined from the experiments. The plasma sheet however is estimated to be several earth radii thick in the work of the Los Alamos Group.

The presence of a field reversal implies the existence of a plasma sheet and an equivelent electrical current associated with the gradient of the field. Recent work by Speiser and Ness (1966) has studied in detail the neutral sheet crossings observed with the IMP-1 satellite and analysis of the observations has yielded the equivalent current necessary to form a physically consistant physical model of the field reversal. These equivelent currents are derived from the curl of the magnetic field with certain limiting assumptions about the sheet geometry. A summary of these currents forming the neutral sheet in the earth's magnetic tail are shown in Figure 17. It is important to note the multiple crossings within a few R_e which have been observed on several orbits and in addition multiple crossings on some orbits (i.e. 45) which occurred 24 hours later. This is interpreted in terms of the diurnal motion of the earth's magnetic dipole axis and the accompanying oscillation of the neutral sheet.

Simultaneous measurements of the flux of energetic electrons and the magnetic field on IMP-1 are shown for orbit number 45 in Figure 18. Beyond the radiation trapping region, large transient fluxes of electrons greater than 45 kev energy are associated with a large scale depression of the magnetic field. Anderson and Ness (1966) refer to this region as the particle cusp. Deeper into the magnetic tail and near the neutral sheet larger fluxes of electrons are observed. Anderson (1965) analyzed the spatial occurrence of these pulses and concluded that they decrease in frequency with increasing distance down the tail axis. Murayama (1966) in an analysis of electron fluxes >160 kev on IMP-1 has not been able to confirm this radial dependency. He concludes that the satellite motion radially is so highly correlated with the motion transverse to the neutral sheet that Anderson's interpretation is spurious. In fact, he finds that the islands tend to occur more frequently closer to the neutral sheet.

From the IMP-1 measurements it is found that the neutral sheet is frequently in motion and also that the field lines have a small component across them connecting the lines on opposite sides of the neutral sheet. This connection or merging of field lines indicates experimental support for the model of the neutral sheet proposed by Axford et al. as opposed to that suggested by Dessler. With one satellite it is difficult to determine a preferred plane of orientation for the neutral sheet. Ness (1965) suggested that the solar magnetospheric equatorial plane is a preferred orientation for the neutral sheet. In this coordinate system, the equatorial plane is defined by the earth-sun line and a unit vector perpendicular to the geomagnetic axis and the earth-sun line. This plane wobbles with a daily nutation of plus and minus 12^{o} superimposed on an annual precession of 23.4^{o} associated with the earth's orbital motion hence an annual variation in inclination of the neutral sheet of $\pm 35^{o}$. As shown on orbit 45 in Figure 18 it is possible for a multiple crossing of the neutral sheet to be observed separated by 24 hours.

For large values of the geomagnetic latitude of the sub-solar point, χ_{ss}, Speiser and Ness (1966) have suggested a tail field geometry which includes the connection of the field lines across a thin but well developed neutral sheet. Vector measurements obtained with IMP-1 have been superimposed when the satellite was within 1 R_e of the noon-midnight meridian plane to guide the interpretation of field line orientation and spacing. This figure illustrates that the neutral sheet will be located above the solar magnetosphere equatorial plane in the summer (and below it in the winter).

In the discussion of the earth's magnetic tail it is also pertinent to mention the oft sought but seldom uniquely measured ring current. Early measurements by satellites indicated the possibility of a ring current and even as recently as 1964, the Electron 2 measurements have been interpreted in terms of such a phenomena (Dolginov et al., 1965). However, with our present view of the neutral sheet and particularly the particle cusp region it now appears that the depression associated with a "ring current" actually occurs for only a limited longitude of the earth between 1800-2400-0600 local time.

In a sketch by Anderson (1966) (Figure 20) he has indicated the relative geometry or topology of the distorted geomagnetic field and the development of regions for particle trapping and the particle cusp region. Omitted is an indication of the connection of field lines across the neutral sheet at distances greater than about 15 R_e as indicated in Figure 19. Note also that in the diagram, lines of force on the sun lit side of the earth near the sub-solar point on the magnetosphere boundary do not support "permanent" trapping of particles.

Particle measurements in the radiation belts have not yet revealed a sufficient intensity to generate the necessary magnetic field associated with storm time ring currents. The results by Hoffman and Bracken (1965) suggest that thus far the particles forming a significant ring current have yet to be directly detected. However, the particles associated with the cusp region and the plasma sheet certainly represent appreciable fluxes whose equivelent currents generate strong perturbing magnetic fields highly distorting the geomagnetic field. The mechanism leading to the development of the earth's magnetic tail is presently under investigation. It is possible that there exists direct connection of interplanetary field lines to the geomagnetic field as originally emphasized by Dungey (1961). It has also been suggested that a type of viscous interaction between the plasma in the magnetosheath and the geomagnetic field drags lines of force back to form the tail (Axford, 1964). Unfortunately, the few measurements which are sufficiently definitive to establish the position of the magnetosphere boundary do not determine locally the surface normal so that a measure of the field component normal to the surface cannot be directly made.

11378

Summary and Prognosis

Satellite measurements of the outer geomagnetic field have revealed the distortion and containment of the geomagnetic field and formation of an external magnetic tail as a result of the flux of the solar wind. In addition there appears to be a permanent detached bow shock wave associated with the super-Alfvénic interaction of the solar plasma with the geomagnetic field. Both the shock wave and magnetopause are frequently in motion. The magnetosheath is a region in which thermalized solar plasma and transient intense fluxes of electrons are observed. It is supposed that there is an active mechanism leading to the development of the acceleration of these particles at or near the shock surface. Details of the earth's neutral sheet indicate frequent fluctuation of its position in the magnetic tail in the absence of any significant magnetic or solar activity. There remain, however, certain major problems in establishing definitive quantitative models of the physical phenomena which have been observed. It can be anticipated that within 10 years after the discovery of the radiation belts, i.e. 1968, that a great wealth of additional experimental data will be available from the recent sophisticated and high data rate satellites such as EGO's and Pioneers providing definitive as well as simultaneous determinations of separate particle, plasma, and field phenomena.

Author

Acknowledgements

It is my pleasure to acknowledge the important participation in the research reported upon here of my colleagues: Dr. D. H. Fairfield, Mr. C. S. Scearce and Mr. Joseph Seek of the Goddard Space Flight Center.

References

Anderson, K. A., 1965, J. Geophys. Res. 70, 4741.

Anderson, K. A., 1966, preprint (March 1966).

Anderson, K. A., H. Harris and R. J. Paoli, 1965, J. Geophys. Res. 70, 1039.

Anderson, K. A. and N. F. Ness, 1966, J. Geophys. Res. 71, 3705.

Axford, W. I., 1962, J. Geophys. Res. 67, 3791.

Axford, W. I., 1964, Planet. Space Science 12, 45.

Axford, W. I., H. E. Petschek and G. L. Siscoe, 1965, J. Geophys.Res., 70, 1231.

Bame, S. J., J. R. Asbridge, H.E. Felthauser, R. A. Olson and I. B. Strong, 1966 Phys. Rev. Letters 16, 138.

Bernstein, W. R., R. W. Fredricks and F. L. Scarf, 1964, J. Geophys. Res. 69 1201.

Bonetti, A., H. S. Bridge, A. J. Lazarus, B. Rossi and F. Scherb, 1963, J. Geophys. Res. 68, 4017.

Bridge, H. S., C. Dilworth, A. J. Lazarus, E. F. Lyon, B. Rossi and F. Scherb, 1962, J. Phys. Soc. Japan 17, A-II, 553.

Bridge, H. S., A. Egidi, A. Lazarus, E. Lyon and L. Jacobson, 1965, Space Research V, 969.

Cahill, L. J., 1964a, I G Bulletin 79, 231.

Cahill, L. J., 1964b, in Space Physics ed. by D. P. LeGalley and A. Rosen, John Wiley and Sons, New York, 301.

Cahill, L. J., 1966, Space Research VI, to appear.

Cahill, L. J. and P. G. Amazeen, 1963, J. Geophys. Res. 68, 1835.

Cain, J. C., I. R. Shapiro, J. D. Stolarik and J. P. Heppner, 1962, J. Geophys. Res. 67. 5055.

Coleman, P. J. Jr., 1964, J. Geophys. Res. 69, 3051.

Coleman, P. J. Jr., L. Davis and C. P. Sonett, 1960a, Phys. Rev. Letters 5, 43.

Coleman, P. J. Jr., C. P. Sonett, D. L. Judge and E. J. Smith, 1960b, J. Geophys. Res. 65, 1856.

Corday, J. G., 1965, J. Geophys. Res. 70, 1278.

Dessler, A. J., 1964, J. Geophys. Res. 69, 3913.

Dessler, A. J. and R. D. Juday, 1965, Planet. Space Science 13, 63.

Dolginov, S. Sh., Ye. G. Yeroshenko. L. N. Zhuzgov, and L. O. Tyurmina, 1960, Space Research I, 863.

Dolginov, S. Sh., Ye. G. Yeroshenko. L. N. Zhuzgov, N. V. Pushkov and L.O. Tyurmina, 1961a, Art. Earth Sat. 3, 4, 5, 490.

Dolginov, S. Sh., Ye. G. Yeroshenko, L. N. Zhuzgov, N. V. Pushkov and L. O. Tyurmina, 1961b, Geomag. and Aero. 1, 21.

Dolginov, S. Sh., Ye. G. Yeroshenko and L. N. Zhuzgov, 1965, Space Research VI, to appear.

Dungey, J., 1961, Phys. Rev. Letters 6, 47.

Fairfield, D. H., N. F. Ness, C. S. Scearce and J. B. Seek, 1966, Trans. AGN 47, 161.

Fan, C. Y., G. Gloeckler and J. A. Simpson, 1966, J. Geophys. Res. 71, 1837.

Fan, C. Y., G. Gloeckler and J. A. Simpson, 1964, Phys. Rev. Letters 13, 149.

Frank, L. A., 1965, J. Geophys. Res. 70, 1593.

Frank, L. A. and J. A. Van Allen, 1964, in Research in Geophysics I, MIT Press, Cambridge, Mass., 161.

Fredricks, R. W., F. L. Scarf and W. Bernstein, 1965, J. Geophys. Res. 70, 21.

Freeman, J. W., 1964, J. Geophys. Res. 69, 1691.

Freeman, J. W., J. A. Van Allen and L. J. Cahill, 1963, J. Geophys, Res. 68,2121.

Heppner, J.P., 1965, GSFC preprint X-612-65-490.

Heppner, J. P., N. F. Ness, T. L. Skillman and C. S. Scearce, 1962, J. Phys.. Soc. Japan 17, A-II, 546.

Heppner, J. P., N. F. Ness, T. L. Skillman and C. S. Scearce, 1963, J. Geophys. Res. 68, 1.

Holzer, R. E., M. E. McLeod and E. J. Smith, 1966, J. Geophys. Res. 71, 1481.

Jokipii, J. R., 1966, J. Geophys, Res. 71, 3173.

Jokipii, J. R. and L. Davis, Jr., 1964, Phys. Rev. Letters 13, 739.

Hoffman, R. A. and P. A. Bracken, 1965, J. Geophys. Res. 70, 3541.

Kellogg, P. J., 1962, J. Geophys, Res. 67, 3805.

McCracken, K. G., 1962, J. Geophys. Res. 67, 447.

Murayama, R., 1966, Enrico Fermi Inst. Dept. EFINS-66-64, University of Chicago.

Ness, N. F., 1965, J. Geophys. Res. 70, 2989.

Ness, N. F., C. S. Scearce and S. Cantarano, 1966, J. Geophys. Res. 71, 3305.

Ness, N. F., C. S. Scearce and J. B. Seek, 1964, J. Geophys. Res. 69, 3531.

Ness, N. F., C. S. Scearce and J. B. Seek, 1966, Trans. AGU 47, 162.

Ness, N. F., C. S. Scearce, J. B. Seek and J. M. Wilcox, 1965, Space Research VI, to appear.

Noerdlinger, P. D., 1964, J. Geophys. Res. 69, 369.

Obayashi, T., 1964, J. Geophys. Res. 69, 861.

Piddington, J. H., 1960, J. Geophys. Res. 65, 93.

Rossi, B., 1963, Space Research III, 529.

Scarf, F. L., W. Bernstein and R. W. Fredricks, 1965, J. Geophys. Res. 70, 9.

Scherb, F., 1964, Space Research IV, 797.

Serbu, P. and E. Maier, 1966, J. Geophys. Res. 71, 3755.

Siscoe, G. L., E. J. Smith, L. Davis, Jr., P. J. Coleman and D. E. Jones, 1966, Trans. AGU 47, 143.

Smith, E. J., 1962, J. Geophys. Res. 67, 2045.

Smith, E. J., P. J. Coleman, D. L. Judge and C. P. Sonett, 1960, J. Geophys. Res. 65, 1858.

Smith, E. J., C. P. Sonett and J. W. Dungey, 1964, J. Geophys. Res, 69, 2669.

Sonett, C. P., 1960, Phys. Rev. Letters 5, 46.

Sonett, C. P., D. L. Judge, A. R. Sims and J. M. Kelso, 1960a, J. Geophys, Res. 65,55.

Sonett, C. P., E. J. Smith, D. L. Judge and P. J. Coleman, 1960b, Phys, Rev. Letters 4, 161.

Sonett, C. P., E. J. Smith and A. R. Sims, 1960c, Space Research I, 921

Speiser T. and N. F. Ness, 1966, J. Geophys, Res. 71, to appear.

Spreiter, J. R. and W. P. Jones, 1963, J. Geopjys. Res. 68, 3555.

Wolfe, J. W., R. W. Silva, and M. A. Myers, 1966a, J. Geophys. Res. 71, 1319.

Wolfe, J. W., R. W. Silva, and M. Myers, 1966b, Space Research VI, to appear.

SATELLITE	LAUNCH DATE	INCLINATION	LIFETIME	RANGE (γ)	SENSITIVITY	DISTANCE
Sputnik 3	5-15-58	65°	30	$<6 \times 10^{4}$	5%	<1.3
Pioneer 1	10-11-58	Earth Impact	1	$<10^{3}$	1%	3.7-7.0
						12.3-14.6
*Lunik I	1-2-59	Solar Orbit	1	<6000	200γ	3-6
Explorer 6	8-7-59	47°	61	$<2 \times 10^{4}$	3%	2-7.5
*Lunik II	9-12-59	Lunar Impact	33.5 hr.	<1500	50γ	3-6
Vanguard 3	9-18-59	33°	85	$10^{4}-6 \times 10^{4}$	4γ	<1.8
Pioneer 5	3-11-60	Solar Orbit	50	$<10^{3}$	$0.05-5\gamma$	5-9
*Explorer 10	3-25-61	33°	2.2	$30-5 \times 10^{3}$	3γ	1.8-7
				$\pm$ 50	0.3γ	6-42.6
*Explorer 12	8-16-61	33°	112	$\pm$ 500	10γ	4-13.5
*Explorer 14	10-3-62	33°	300	$\pm$ 250	5γ	5-16.5
Alouette	9-29-62	80°	S.O.	$<6 \times 10^{4}$	0.3%	1.17
Explorer 15	10-27-62	18°	90	$\pm$ 4000	40γ	1.7-4.0
*Explorer 18				<300	$\pm$ 0.25	<32
(IMP I)	11-27-63	33°	181	<40		
*Electron 2	1-30-64	61°	90	<120	2γ	3-11.6
				<1200	20γ	
Cosmos 26	3-18-64	49°	194	$<7 \times 10^{4}$	$\pm 4\gamma$	~1.05
*Electron 4	7-11-64	61°	?	<240	?	3-11.4
				<1200		
*OGO-1	9-5-64	31°	S.O.	<500	$\pm 3\gamma$	3.8-24.3
*Explorer 21	10-4-64	34°	150	<300	$\pm 0.25\gamma$	6-15.9
(IMP II)				<40		
Cosmos 49	10-24-64	49°	?	$<7 \times 10^{4}$	$\pm 4\gamma$	~1.05
*Mariner 4	11-28-64	Solar Orbit	270	<370	$\pm 0.7\gamma$	>10
Explorer 26	12-21-64	20°	S.O.	$<2 \times 10^{3}$	$\pm 2\gamma$	2.5-5.1
*Explorer 28	5-29-65	33°	S.O.	<300	$\pm 0.25\gamma$	<42
(IMP III)				<40		
*OGO 2	10-14-65	87.4°	S.O.	$<8 \times 10^{4}$	$\pm 0.1\gamma$	~1.15
*Pioneer 6	12-16-65	Solar Orbit	S.O.	<64	$\pm 0.25\gamma$	>8

Table 1. Summary of U.S. and U.S.S.R. satellites and space probes that have provided data on the geomagnetic field. (* indicates experiment repetoire included plasma detector)

SATELLITE	LAUNCH DATE	INCLINATION	LIFETIME	RANGE (γ)	SENSITIVITY	DISTANCE
*Lunik 10	3-31-66	Lunar Orbit	60	?	?	<60
*OGO 3	6-6-66	31°	S.O.	$<1.5 \times 10^4$	?	2.1-
				<500	$\pm$ 0.25γ	
*Explorer 33	7-1-66	6° - 28°	S.O.	<200	$\pm$ 0.2γ	8 - 80
*Pioneer 7	8-17-66	Solar Orbit	S.O.	<32	$\pm$ 0.12γ	>12

Inclination - Orbital plane relative to equator
Lifetime - Days (S.O. = Still Operating)
Range - Dynamic range of instrumentation in gammas ($1\ \gamma = 10^{-5}$ oersted)
Sensitivity - Not accuracy
Distance - Geocentric distance range in earth radii ($1\ R_e = 6378.12$ km)

Table 1 (con't)

FIGURE CAPTIONS

Figure 1. Projection on the ecliptic plane of the trajectories of satellites and space probes which investigated the solar wind interaction with the geomagnetic field prior to 1963. The position of the boundary of the regular geomagnetic field and the detached collisionless bow shock wave are shown as known at present. The position of the moon is shown in proper scale as measured in earth radii (R_e).

Figure 2. Particle and magnetic field measurements with Explorer 12 on the in-bound pass of September 13, 1961. These data illustrate the termination of the geomagnetic field at a geocentric distance of 52,000 km (= 8.2 R_e) and an enhanced flux of electrons between 1 and 10 kev beyond forming the quasi-thermalized solar plasma (Freeman, Van Allen, and Cahill, 1963).

Figure 3. Energetic particles measurements obtained with Explorer 12 in 1961 by Freeman (1964). The relative positions of the various regions surrounding the earth defined by the flux intensity of energetic electrons are projected onto the earth's equatorial plane. These include the classical radiation belts as well as the quasi-thermalized plasma forming the magnetosheath.

Figure 4. Simplified diagram of the geomagnetic field as distorted by the solar wind in the noon-midnight magnetic meridian plane according to space investigations prior to 1963. The "inner" and "outer" radiation belts are also shown.

Figure 5. Presentation of same trajectory data as in Figure 1 for satellite and space probe investigations since 1963.

Figure 6. Magnetic field results on out-bound orbit number 1 of the IMP-I satellite 27 November 1963. Note the termination of the regular geomagnetic field at 11.3 R_e and the decrease in magnitude and rapid fluctuations of the magnetic field at 16.8 R_e, identified as the collisionless bow shock wave (Ness et al., 1965).

Figure 7. Measurements of the flux of electrons with energy greater than 45 kev on in-bound orbit number 1 of IMP-I 3 December 1963 showing coincidence of trapping region boundary with magnetopause at 10.8 R_e. Note also the occurrence of intense transient pulses of electron fluxes beyond the magnetopause and within the magnetosheath.

Figure 8. Comparison of the IMP-I rectified boundary crossings with a high speed gas dynamic shock model of Spreiter and Jones (1962). The stand-off ratio or equivalently the specific heat ratio has been adjusted to match the observations. The predicted shape of the shock is seen to be rather closely matched by observations. Also included is the Explorer 10 trajectory, as rotated about the earth-sun line.

Figure 9. Magnetic field and thermal plasma flux measurements obtained with the IMP-II satellite on orbits 8 and 22 in October and November 1965. Identified are the magnetosphere and shock wave boundary crossings on the basis of magnetic field fluctuations as measured by δX_{se} and the magnitude of the magnetic field. (Fairfield et al., 1966)

Figure 10. Ion spectra in the magnetosheath obtained with three different satellites in October 1964 (Wolfe, et al., 1966). The thermalization of the solar wind plasma flux is large since the same instruments generally detect solar plasma in only one or two energy "channels." The relative position of the satellites is shown in the right side of the diagram.

Figure 11. Short time resolution fluxgate magnetometer measurements at the bow shock with the OGO-I satellite in 1964 (Heppner, 1965). Clearly evident is the 12-second satellite spin modulation of the field magnetic field as measured on the Y axis of the instrument. The amplitude of the spin modulation and higher frequency noise superimposed on the wave form increase substantially at and near the shock wave which is detected at 00:02:11.

Figure 12. High frequency search coil magnetometer data from the OGO-I satellite in 1964 out-bound on orbit 36 (Holzer, et al., 1966). Note the traversals of the bow shock wave at 1912 and 1924. Note also the presence of a small but detectable 12-second period fluctuation due to spin modulation in the X, Y, Z channels.

Figure 13. Observations of the termination of the geomagnetic field and the bow shock wave near the sun set terminator by Pioneer 6 on December 16, 1965. The magnetopause is detected at 12.8 R_e and is identified by the magnitude decrease and rms deviation (δD_1) increase. The noise level within the magnetosheath is an order of magnitude higher than the interplanetary and magnetosphere levels and increases near the shock at 20.5 R_e. (Ness et al., 1966).

Figure 14. Projection of the magnetopause and shock wave positions as observed by the IMP-3 satellite in 1965. Note the non-symmetrical position of the magnetopause and shock wave boundaries with respect to the earth-sun line. The asymmetry is in the proper sense for interpretation as the aberration effect on the direction of solar plasma flow due to the helio-centric motion of the earth. (Ness et al., 1966).

Figure 15. Schematic diagram of the night side of the geomagnetosphere. The solar wind interaction with the geomagnetic field extends the field from the polar caps to form a magnetic tail and embedded neutral sheet. The lower figure illustrates a magnetosphere model in which magnetic merging is negligible across the neutral sheet (Dessler and Juday, 1965). The upper figure is one in which merging is appreciable and the development of an enhanced plasma sheet in the magnetic tail is predicted (Axford et al.,1965).

Figure 16. Measurements of the earth's magnetic tail field near the midnight meridian plane by IMP-I on orbit number 41 in early May 1964. The direction of the field is observed to parallel the earth-sun line with a rapid change from anti-solar to solar directed when in-bound at a radial distance of 16 R_e. This is interpreted to represent traversal of the magnetic neutral sheet in the earth's magnetic tail and is characteristic of multiple observations of this phenomena by IMP-I (Ness, 1965).

Figure 17. Projection of the equivalent current vector per unit length from for the earth's neutral sheet crossings obtained by the IMP-I satellite in early 1964 (Speiser and Ness, 1966). The tail of the arrow indicates the satellite position as projected

on to the X-Y solar magnetosphere equatorial plane and the length indicates the magnitude. Note several multiple crossings of the neutral sheet on one orbital pass, such as orbit 45.

Figure 18. Correlation of energetic electron flux and magnetic field measurements obtained on orbit number 45 of the IMP-I satellite in May 1964. A decrease in the magnetic field strength is observed across the multiple neutral sheet crossings which occur between 25-27 R_e. Only very weak fluxes of electrons with energy greater than 45 kev are observed. During this time the satellite moved 2.5 R_e perpendicular to the solar magnetosphere equatorial plane. Twenty-four hours later, multiple neutral sheet crossings were again observed between 17-18 R_e. Note the decrease of field strength below that expected between 8-12 R_e and the accompanying fluctuations of intense particle fluxes.

Figure 19. Suggested neutral sheet and geomagnetic tail field configuration for large "angle of attack" of the solar wind interaction with the geomagnetic field as measured by χ_{ss} . The projection in the noon-midnight meridian plane includes vector measurements obtained within the earth's magnetic tail by the IMP-I satellite in 1964. Neutral sheet crossings on orbits 44 and 45 indicated by dots are also shown. (Speiser and Ness, 1966).

Figure 20. Representation of the solar wind interaction with the geomagnetic field in the noon-midnight meridian plane (Anderson, 1966). The radiation belts are shown as consisting of a stable trapping zone confined within field lines of up to approximately $70^{\circ} \pm 5^{\circ}$

latitude although a strong day-night asymetry exists. In addition a particle tail or cusp region is defined on the night side of the earth in which particle motion is controlled by a highly inflated dipolar magnetic field.

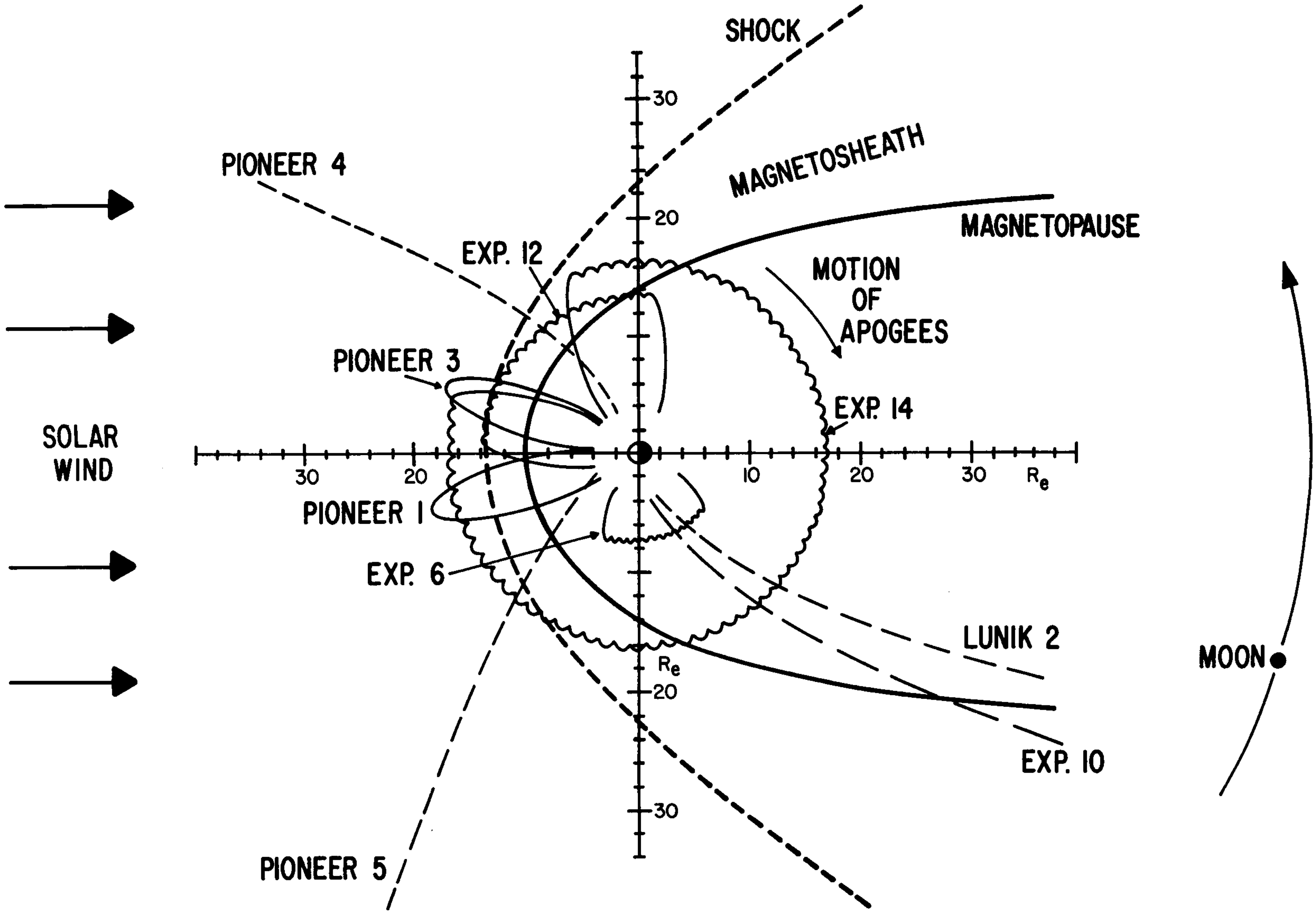
SHOCK
MAGNETOSHEATH
MAGNETOPAUSE
PIONEER 4
EXP. 12
MOTION
OF
APOGEES
PIONEER 3
EXP. 14
SOLAR
WIND
30
20
10
30
20
10
20
30
R_e
20
30
R_e
PIONEER 1
EXP. 6
LUNIK 2
MOON
EXP. 10
PIONEER 5

Figure 1

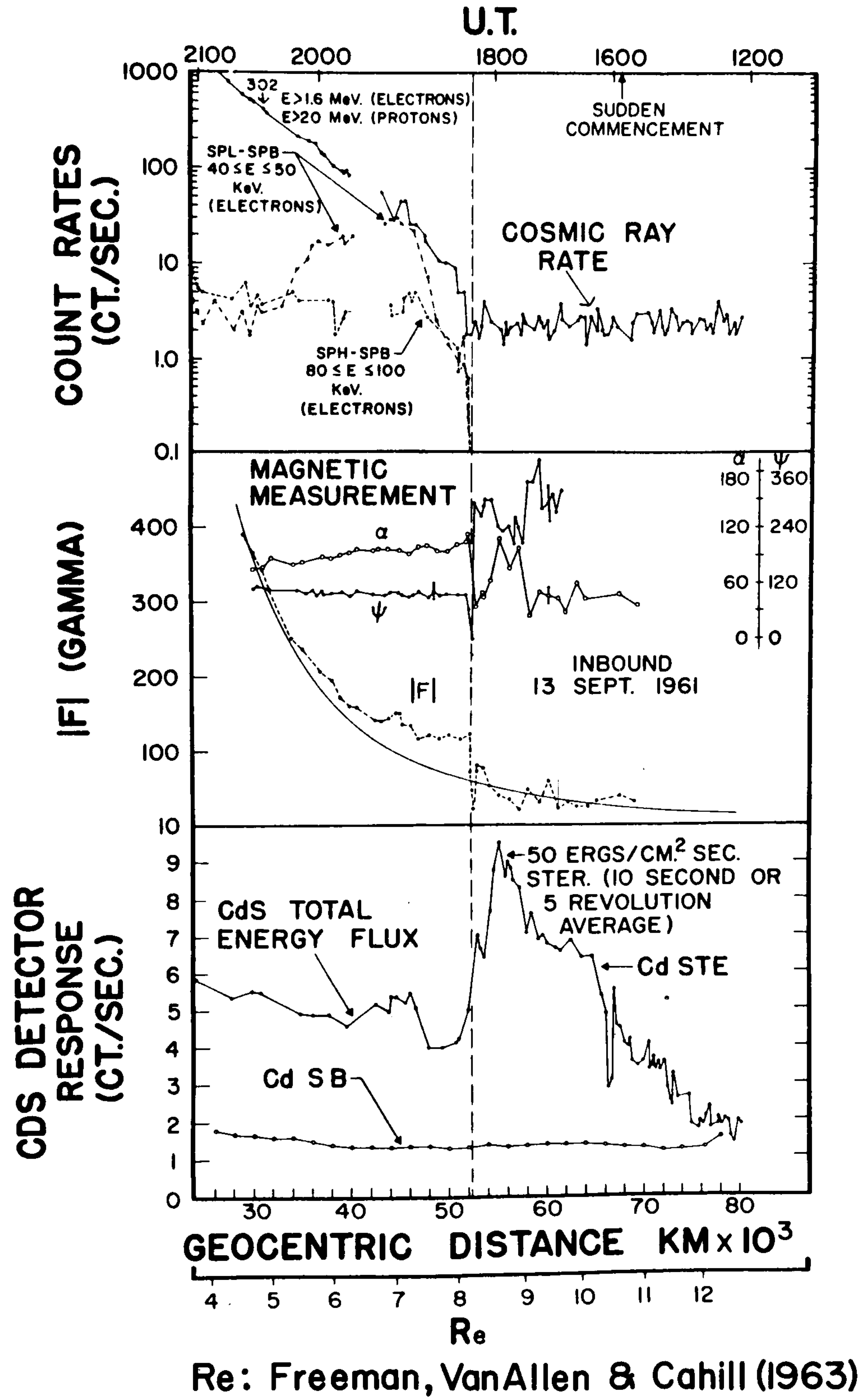

U.T.
2100
2000
1800
1600
1200
1000
100
10
1.0
0.1
COUNT RATES (CT./SEC.)
302
E>1.6 MeV. (ELECTRONS)
E>20 MeV. (PROTONS)
SUDDEN COMMENCEMENT
SPL-SPB 40 ≤ E ≤ 50 KeV. (ELECTRONS)
COSMIC RAY RATE
SPH-SPB 80 ≤ E ≤ 100 KeV. (ELECTRONS)
MAGNETIC MEASUREMENT
α
ψ
|F|
|F| (GAMMA)
400
300
200
100
10
180
120
60
0
360
240
120
0
INBOUND
13 SEPT. 1961
←50 ERGS/CM.² SEC. STER. (10 SECOND OR 5 REVOLUTION AVERAGE)
CdS TOTAL ENERGY FLUX
←Cd STE
Cd SB
CDS DETECTOR RESPONSE (CT./SEC.)
9
8
7
6
5
4
3
2
1
0
30
40
50
60
70
80
GEOCENTRIC DISTANCE KM x 10³
4
5
6
7
8
9
10
11
12
Re
Re: Freeman, VanAllen & Cahill (1963)

Figure 2

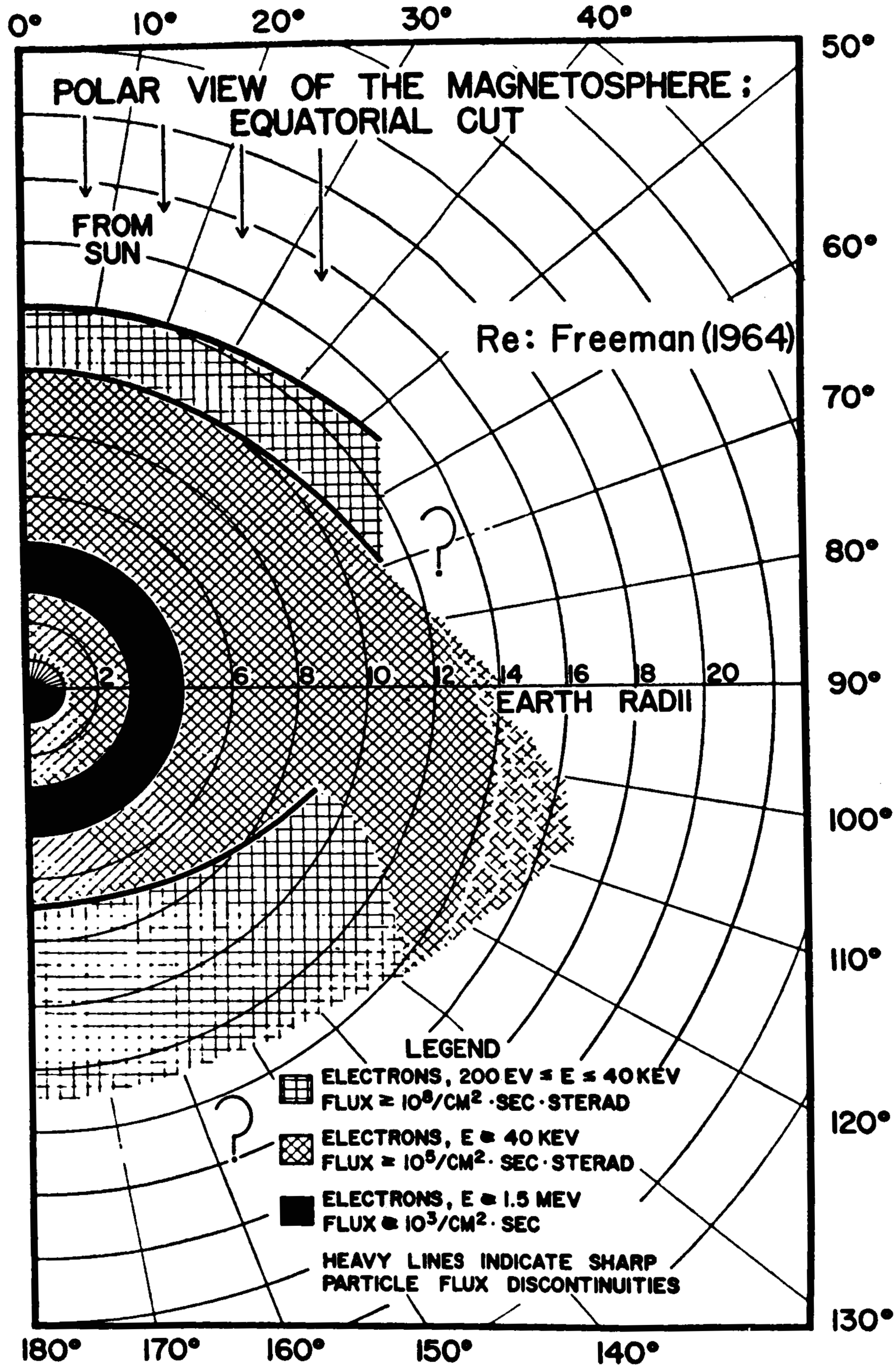
POLAR VIEW OF THE MAGNETOSPHERE; EQUATORIAL CUT
FROM SUN
Re: Freeman (1964)
0°
10°
20°
30°
40°
50°
60°
70°
80°
90°
100°
110°
120°
130°
140°
150°
160°
170°
180°
2
6
8
10
12
14
16
18
20
EARTH RADII
?
?
LEGEND
ELECTRONS, 200 EV ≤ E ≤ 40 KEV
FLUX ≥ 10⁸/CM²·SEC·STERAD
ELECTRONS, E ≥ 40 KEV
FLUX ≥ 10⁵/CM²·SEC·STERAD
ELECTRONS, E ≥ 1.5 MEV
FLUX ≥ 10³/CM²·SEC
HEAVY LINES INDICATE SHARP PARTICLE FLUX DISCONTINUITIES

Figure 3

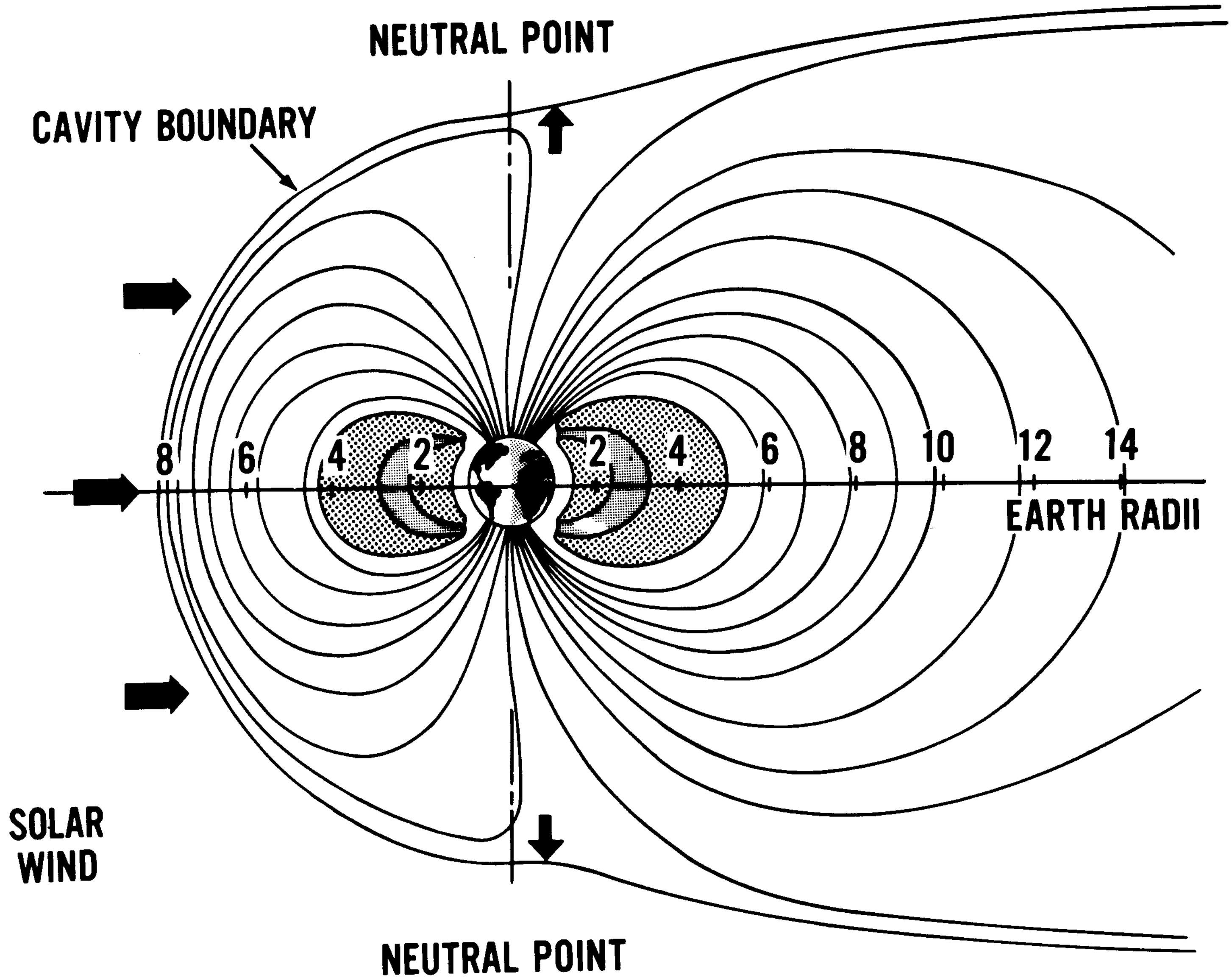
NEUTRAL POINT
CAVITY BOUNDARY
8
6
4
2
2
4
6
8
10
12
14
EARTH RADII
SOLAR
WIND
NEUTRAL POINT

Figure 4

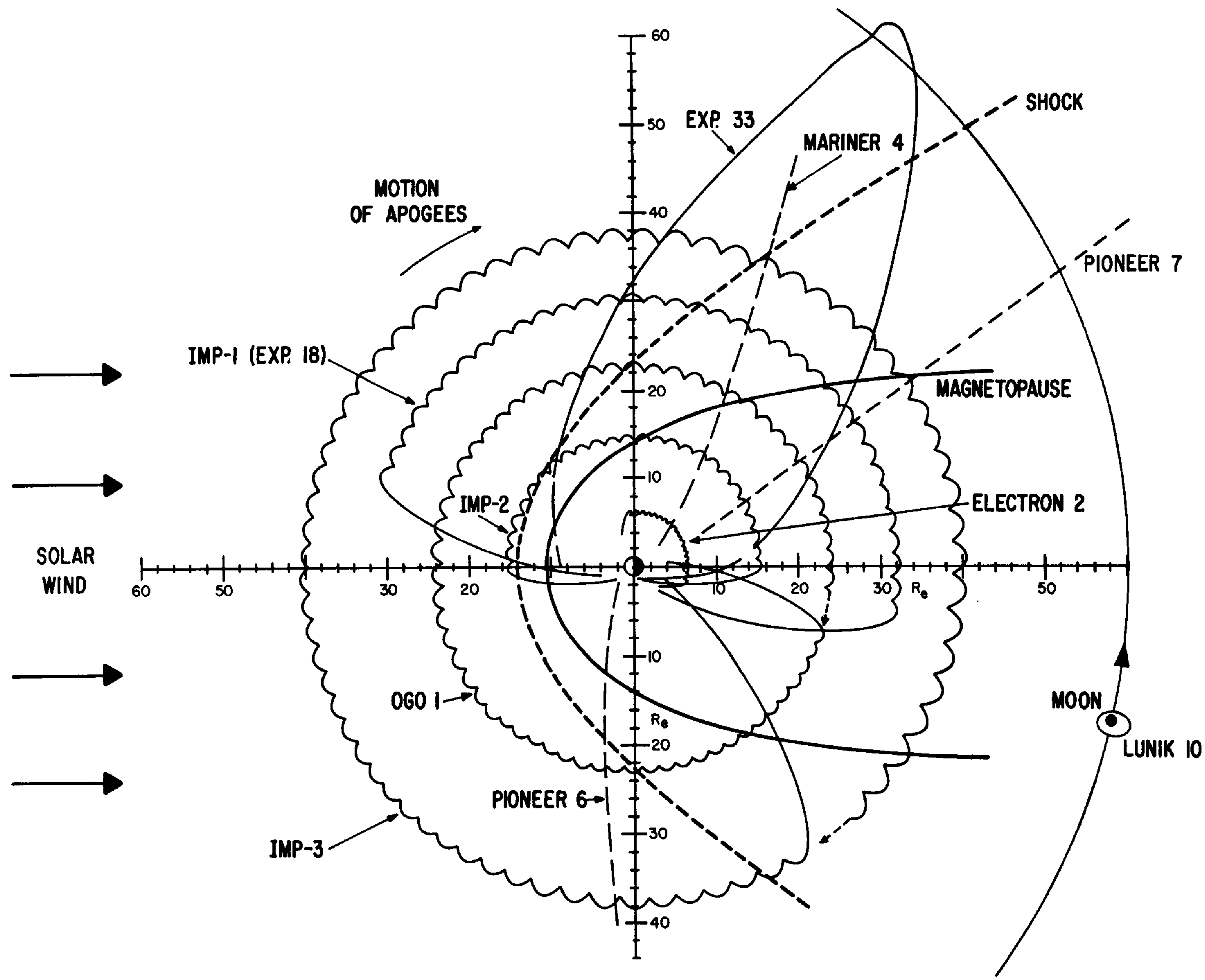
SOLAR
WIND
MOTION
OF APOGEES
IMP-I (EXP. 18)
IMP-2
OGO I
PIONEER 6
IMP-3
EXP. 33
MARINER 4
SHOCK
PIONEER 7
MAGNETOPAUSE
ELECTRON 2
MOON
LUNIK 10
R_e
60
50
40
30
20
10

Figure 5

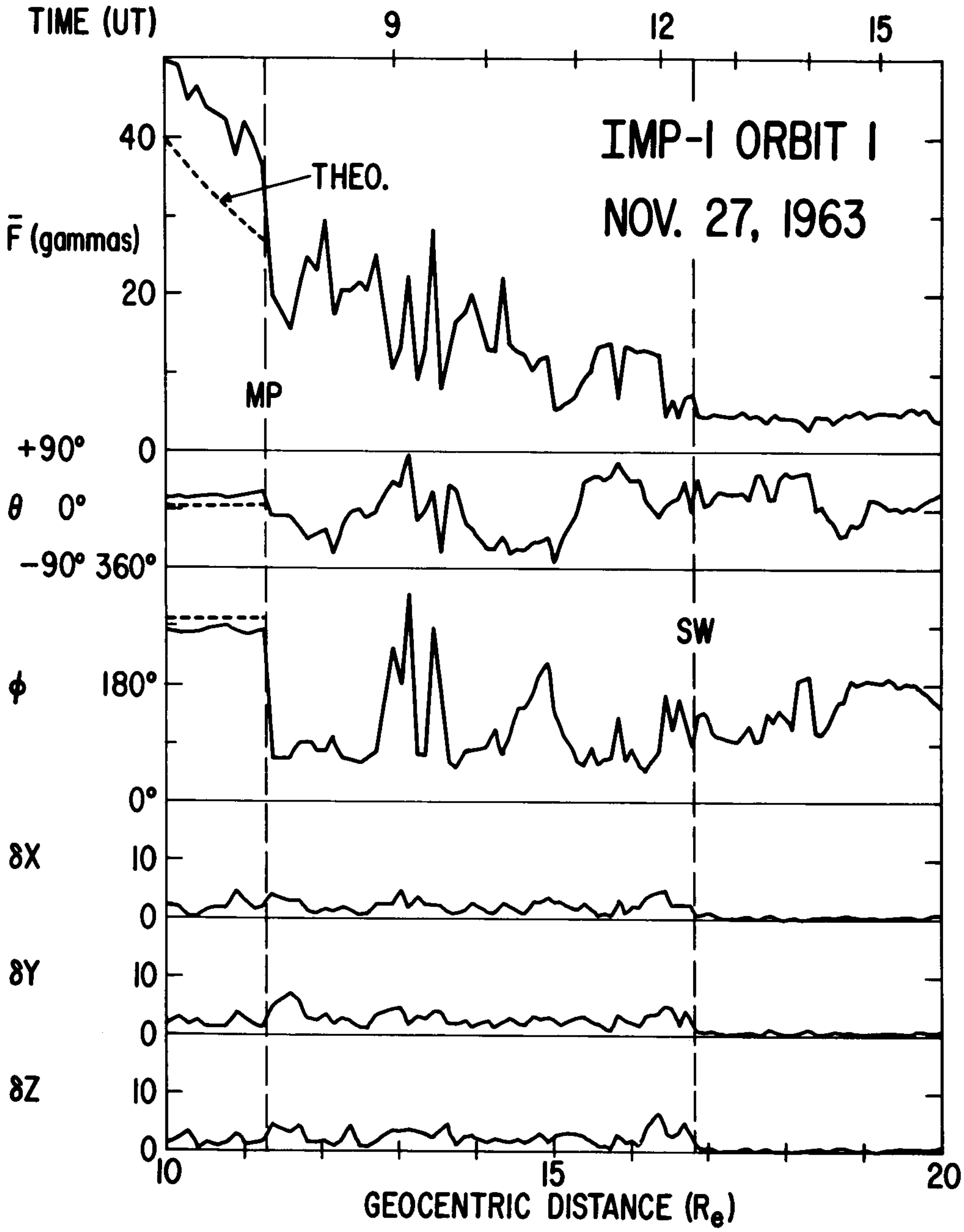
TIME (UT)
9
12
15
IMP-I ORBIT I
NOV. 27, 1963
THEO.
F̄ (gammas)
40
20
0
MP
+90°
θ 0°
-90° 360°
SW
φ
180°
0°
δX
10
0
δY
10
0
δZ
10
0
10
15
20
GEOCENTRIC DISTANCE (R_e)

Figure 6

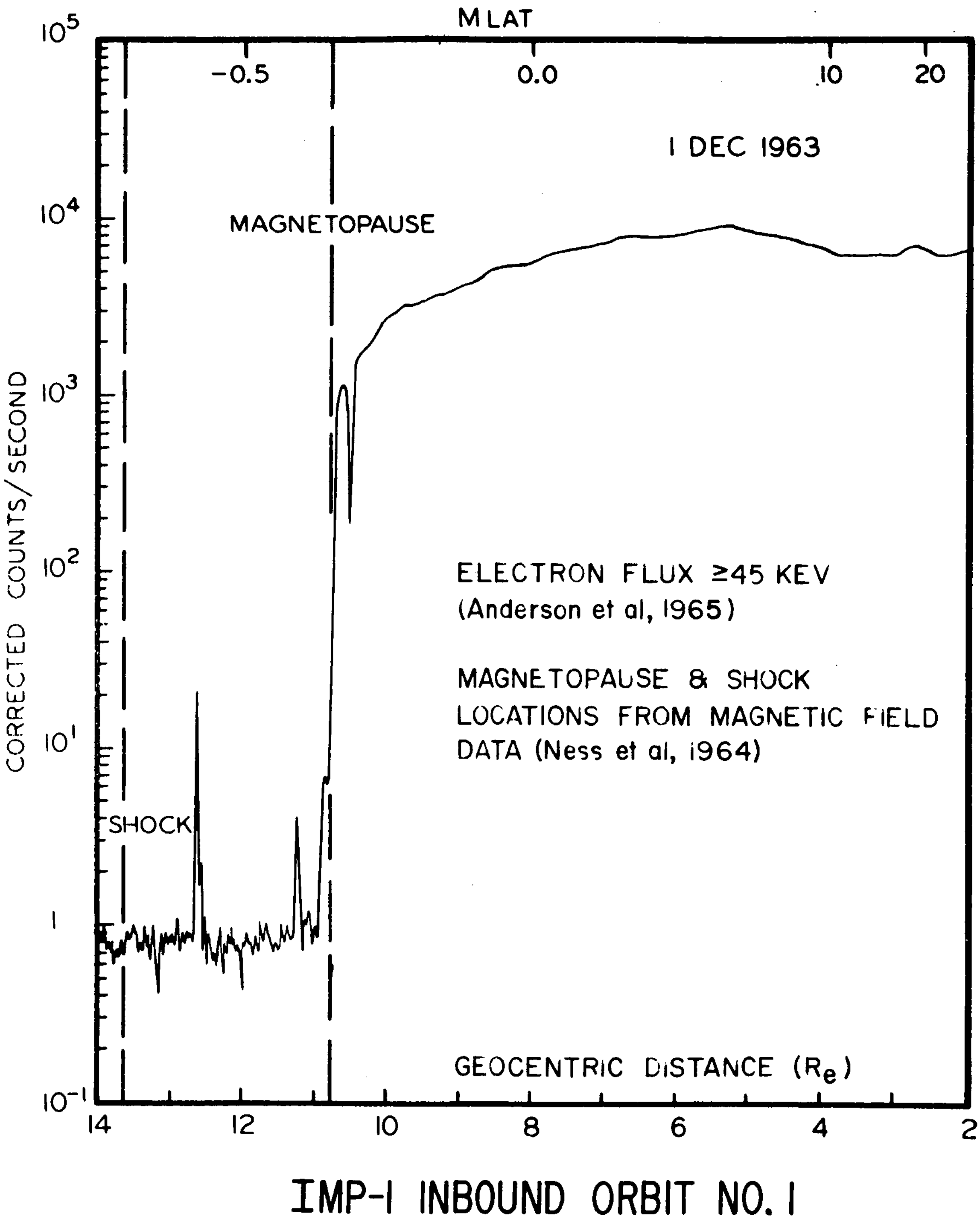

M LAT
−0.5
0.0
.10
20
1 DEC 1963
MAGNETOPAUSE
SHOCK
ELECTRON FLUX ≥45 KEV
(Anderson et al, 1965)
MAGNETOPAUSE & SHOCK
LOCATIONS FROM MAGNETIC FIELD
DATA (Ness et al, 1964)
CORRECTED COUNTS/SECOND
10^5
10^4
10^3
10^2
10^1
1
10^{-1}
GEOCENTRIC DISTANCE (R_e)
14
12
10
8
6
4
2
IMP-1 INBOUND ORBIT NO. 1

Figure 7

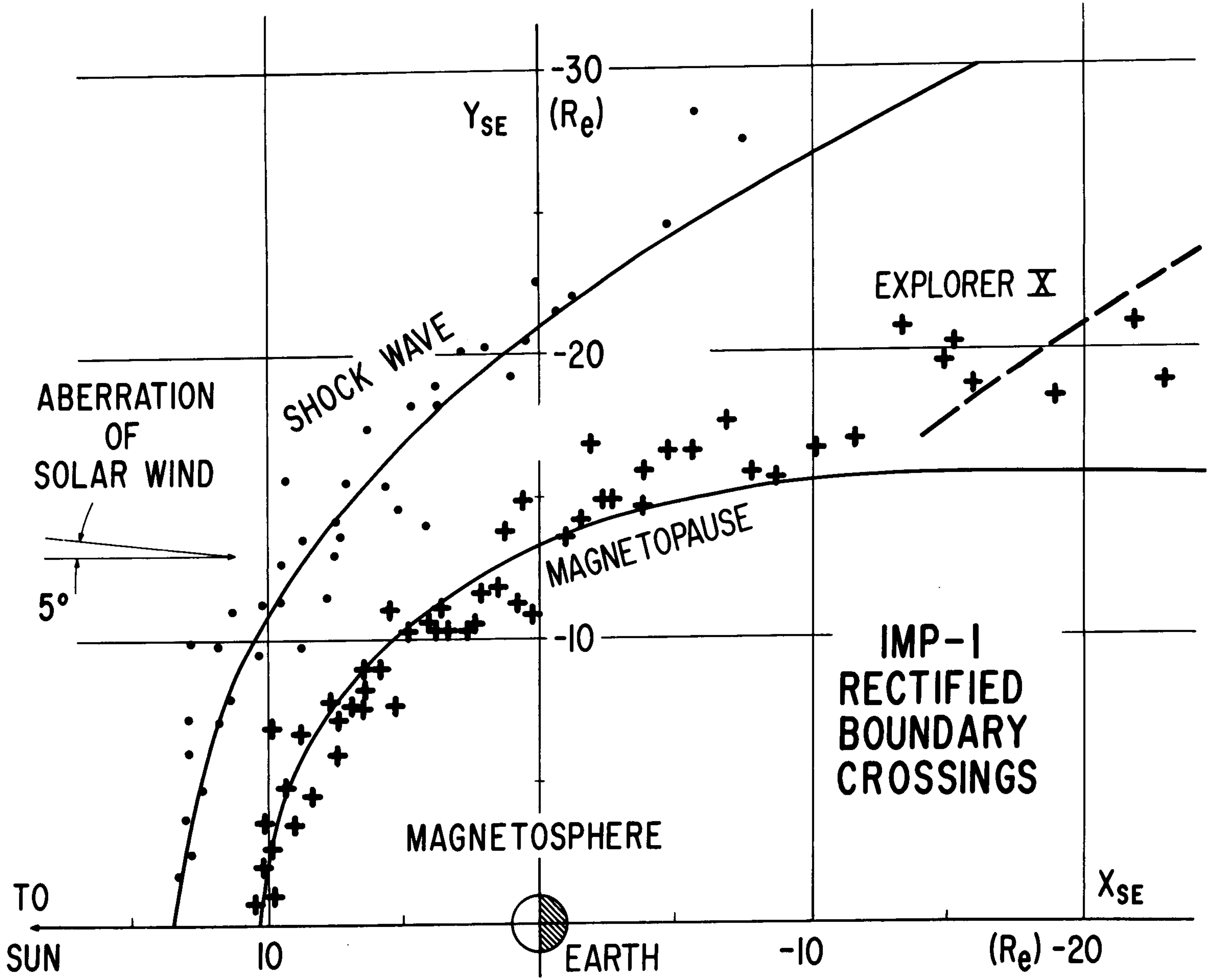

Y_{SE}
-30
(R_e)
-20
-10
SHOCK WAVE
ABERRATION
OF
SOLAR WIND
5°
MAGNETOPAUSE
MAGNETOSPHERE
EXPLORER X
IMP-I
RECTIFIED
BOUNDARY
CROSSINGS
TO
SUN
10
EARTH
-10
(R_e) -20
X_{SE}

Figure 8

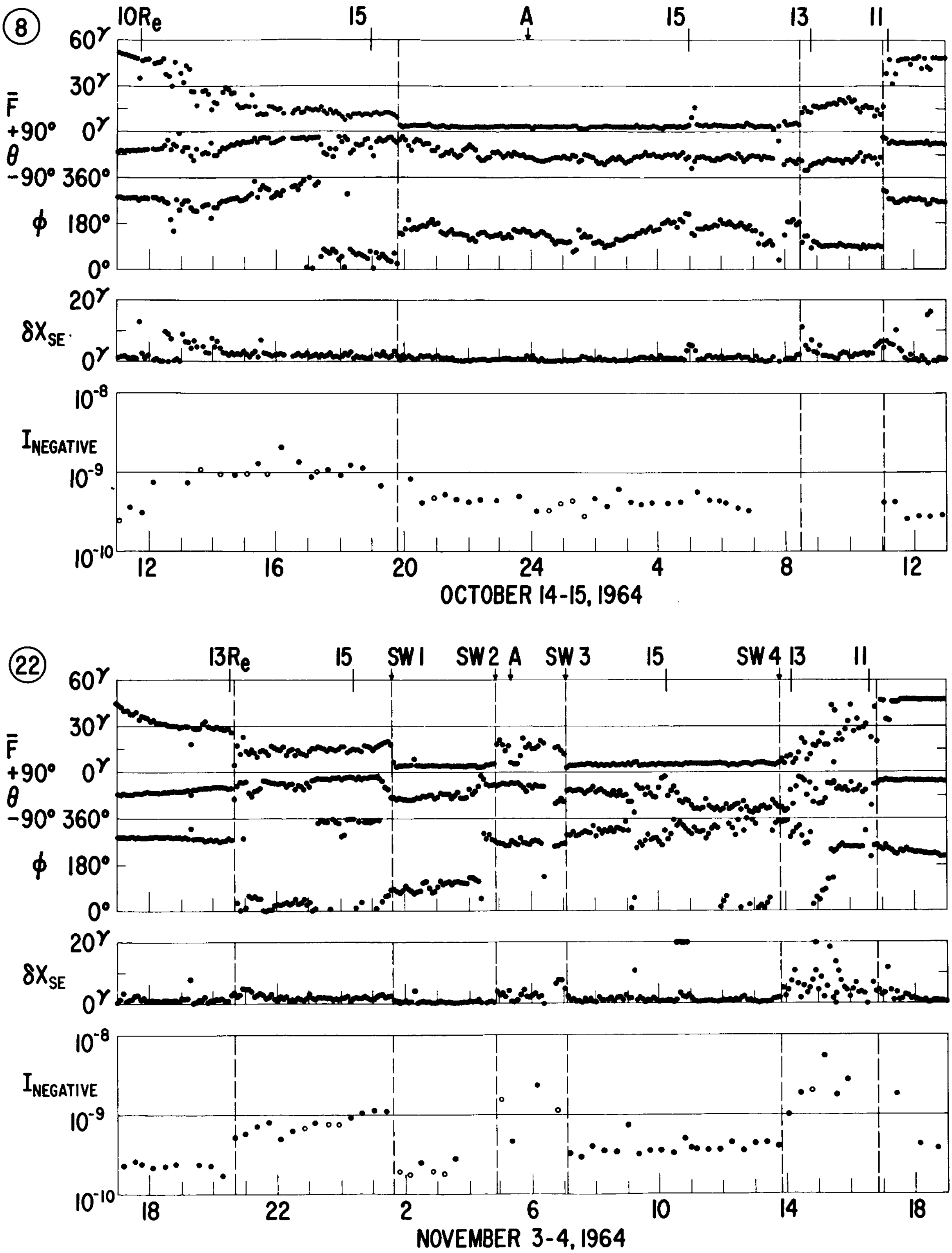
8
10Re
15
A
15
13
11
60γ
30γ
F̄
+90°
0γ
θ
-90° 360°
φ
180°
0°
20γ
δXSE
0γ
10-8
INEGATIVE
10-9
10-10
12
16
20
24
4
8
12
OCTOBER 14-15, 1964
22
13Re
15
SW1
SW2
A
SW3
15
SW4
13
11
18
22
2
6
10
14
18
NOVEMBER 3-4, 1964

Figure 9

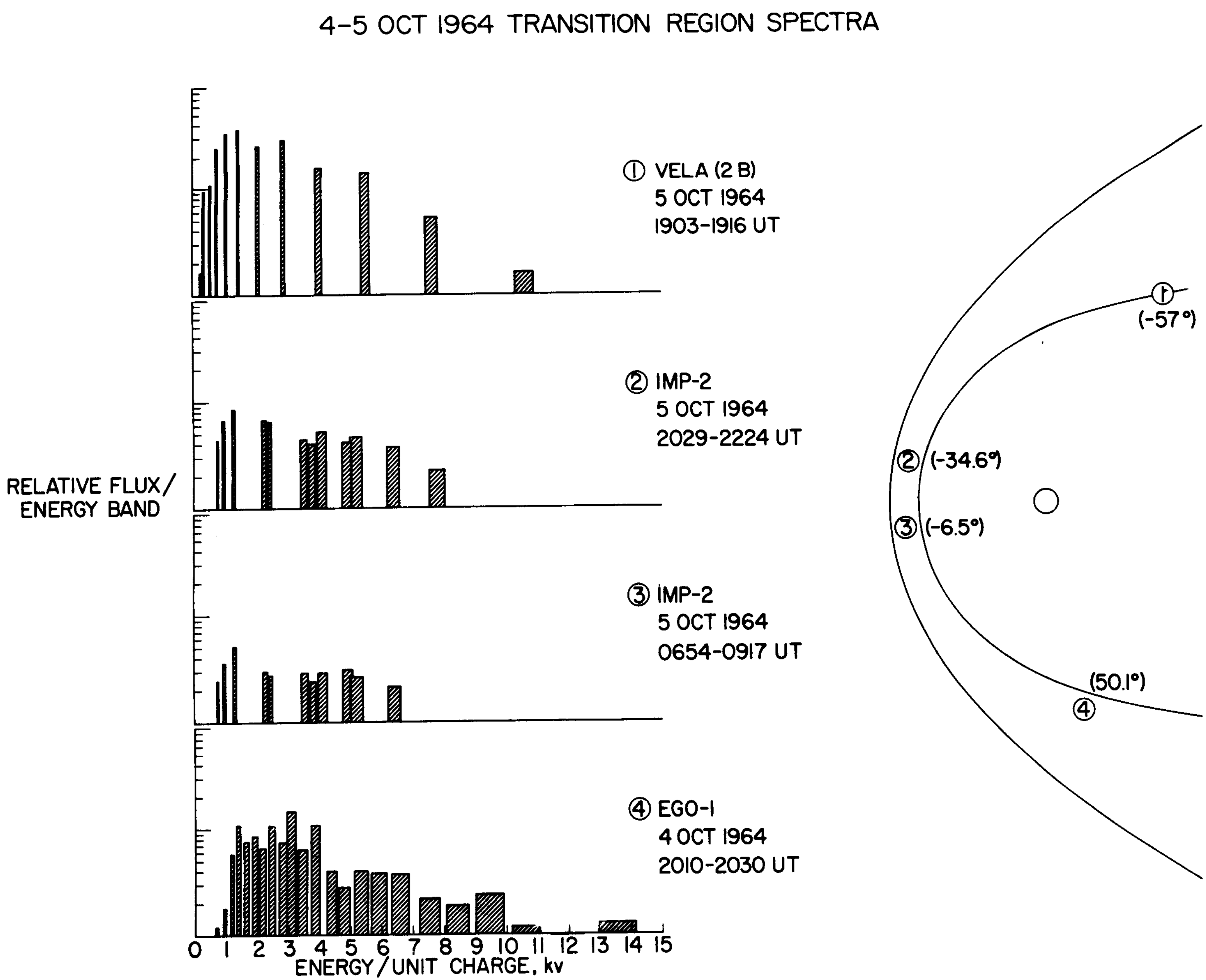
4-5 OCT 1964 TRANSITION REGION SPECTRA
RELATIVE FLUX/
ENERGY BAND
① VELA (2 B)
5 OCT 1964
1903-1916 UT
② IMP-2
5 OCT 1964
2029-2224 UT
③ IMP-2
5 OCT 1964
0654-0917 UT
④ EGO-1
4 OCT 1964
2010-2030 UT
0 1 2 3 4 5 6 7 8 9 10 11 12 13 14 15
ENERGY/UNIT CHARGE, kv
① (-57°)
② (-34.6°)
③ (-6.5°)
④ (50.1°)

Figure 10

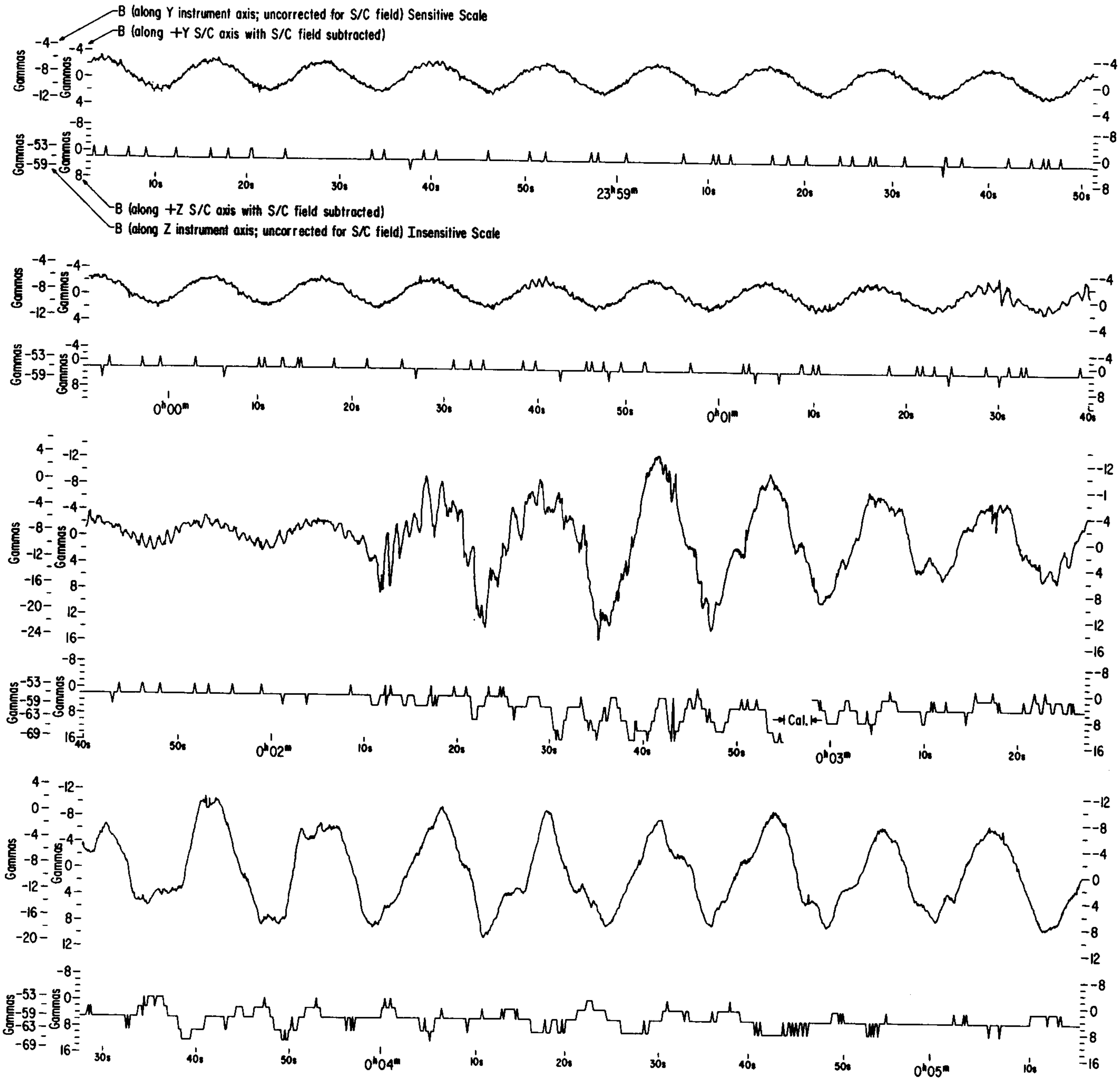

B (along Y instrument axis; uncorrected for S/C field) Sensitive Scale
B (along +Y S/C axis with S/C field subtracted)
B (along +Z S/C axis with S/C field subtracted)
B (along Z instrument axis; uncorrected for S/C field) Insensitive Scale
Gammas
23h59m
0h00m
0h01m
0h02m
0h03m
0h04m
0h05m
Cal.

Figure 11

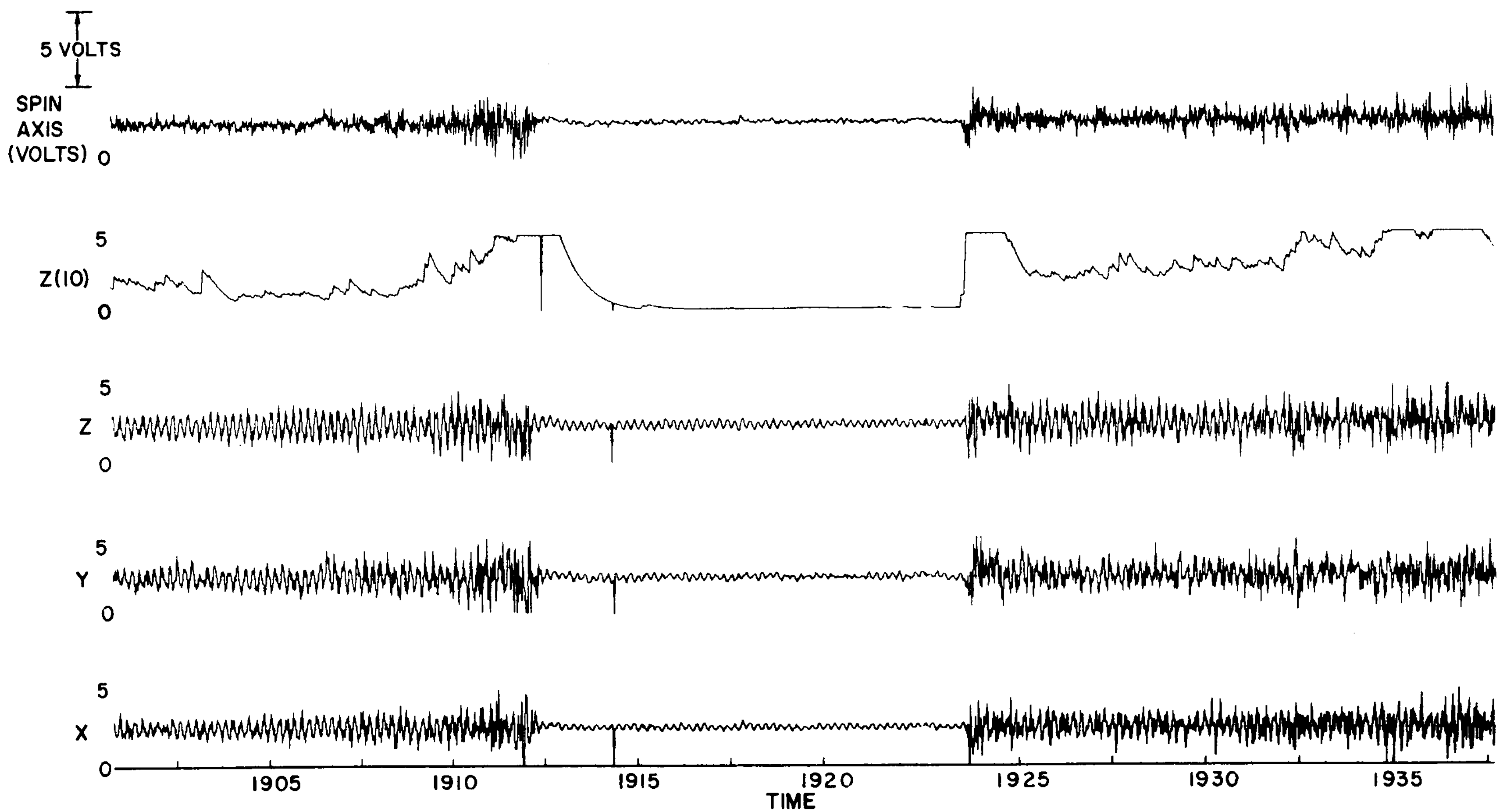
5 VOLTS
SPIN
AXIS
(VOLTS)
0
5
Z(10)
0
5
Z
0
5
Y
0
5
X
0
1905
1910
1915
1920
1925
1930
1935
TIME

Figure 12

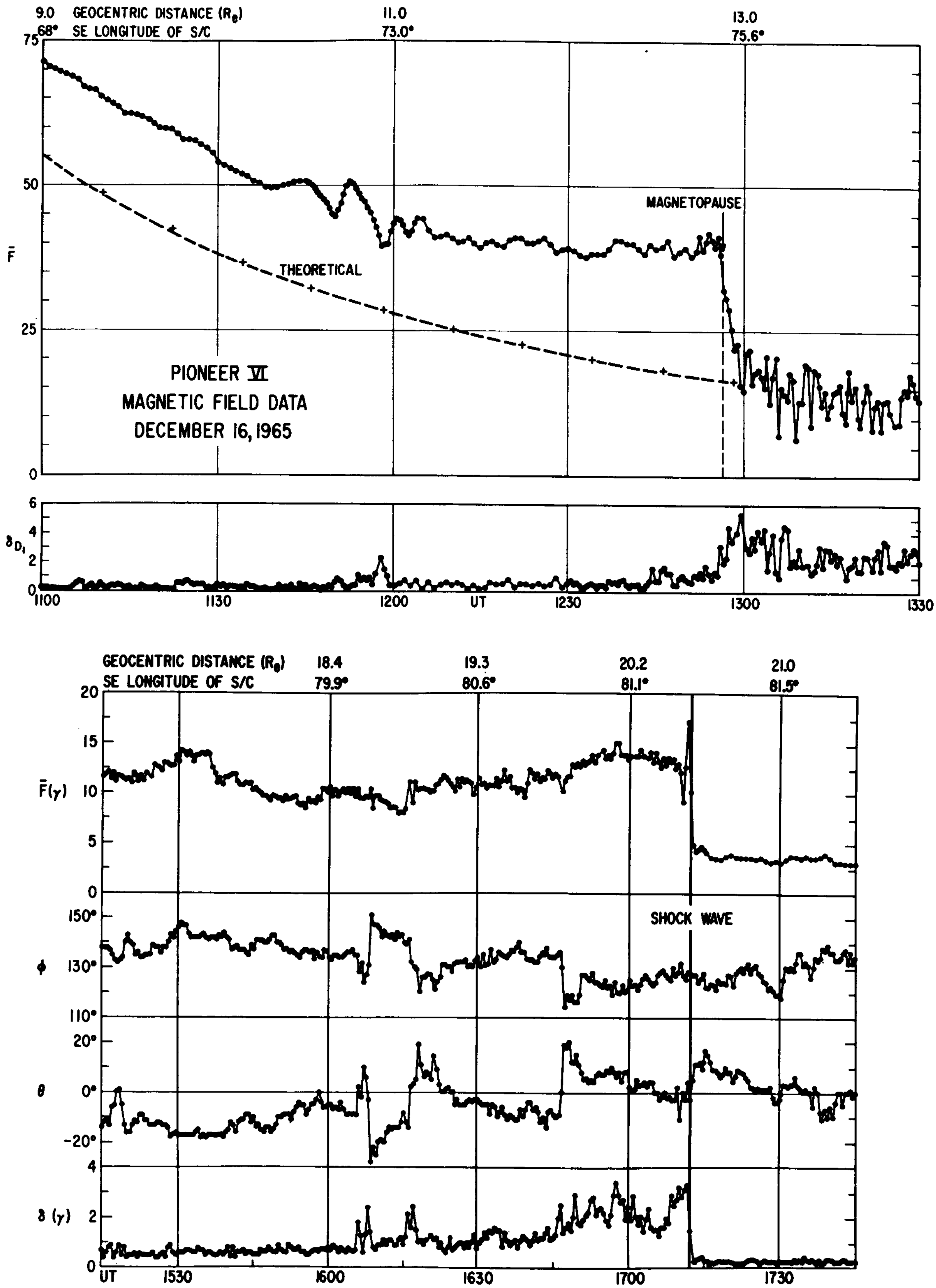

9.0 GEOCENTRIC DISTANCE (R_e)
68° SE LONGITUDE OF S/C
11.0
73.0°
13.0
75.6°
75
50
25
0
$\bar{F}$
MAGNETOPAUSE
THEORETICAL
PIONEER VI
MAGNETIC FIELD DATA
DECEMBER 16, 1965
6
4
2
0
δ_{D_1}
1100
1130
1200
UT
1230
1300
1330
GEOCENTRIC DISTANCE (R_e)
SE LONGITUDE OF S/C
18.4
79.9°
19.3
80.6°
20.2
81.1°
21.0
81.5°
20
15
10
5
0
$\bar{F}(\gamma)$
150°
130°
110°
ϕ
SHOCK WAVE
20°
0°
-20°
θ
4
2
0
$\delta(\gamma)$
UT
1530
1600
1630
1700
1730

Figure 13

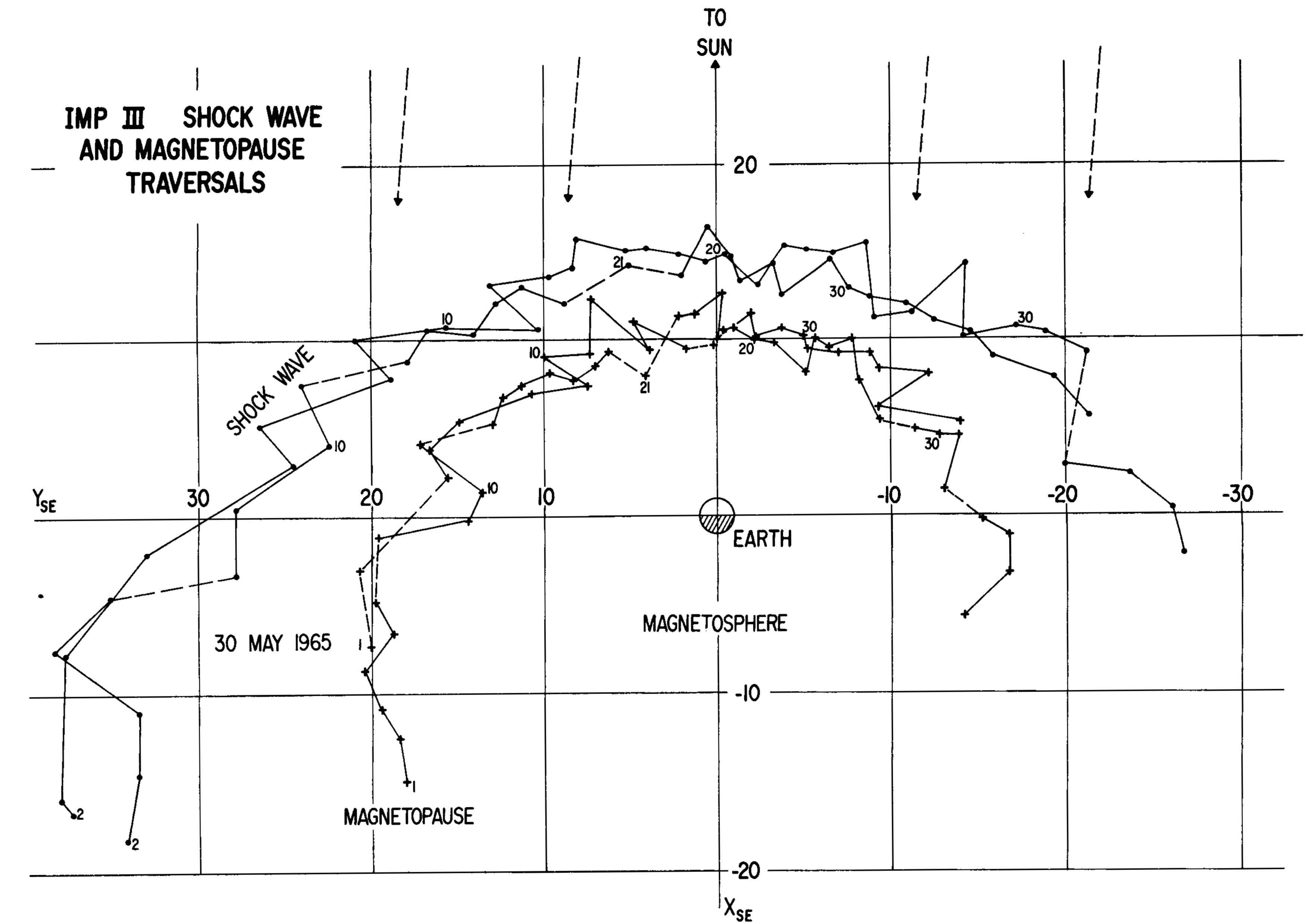
IMP III SHOCK WAVE
AND MAGNETOPAUSE
TRAVERSALS
TO
SUN
20
-10
-20
Y_{SE}
30
20
10
-10
-20
-30
X_{SE}
EARTH
MAGNETOSPHERE
SHOCK WAVE
MAGNETOPAUSE
30 MAY 1965

Figure 14

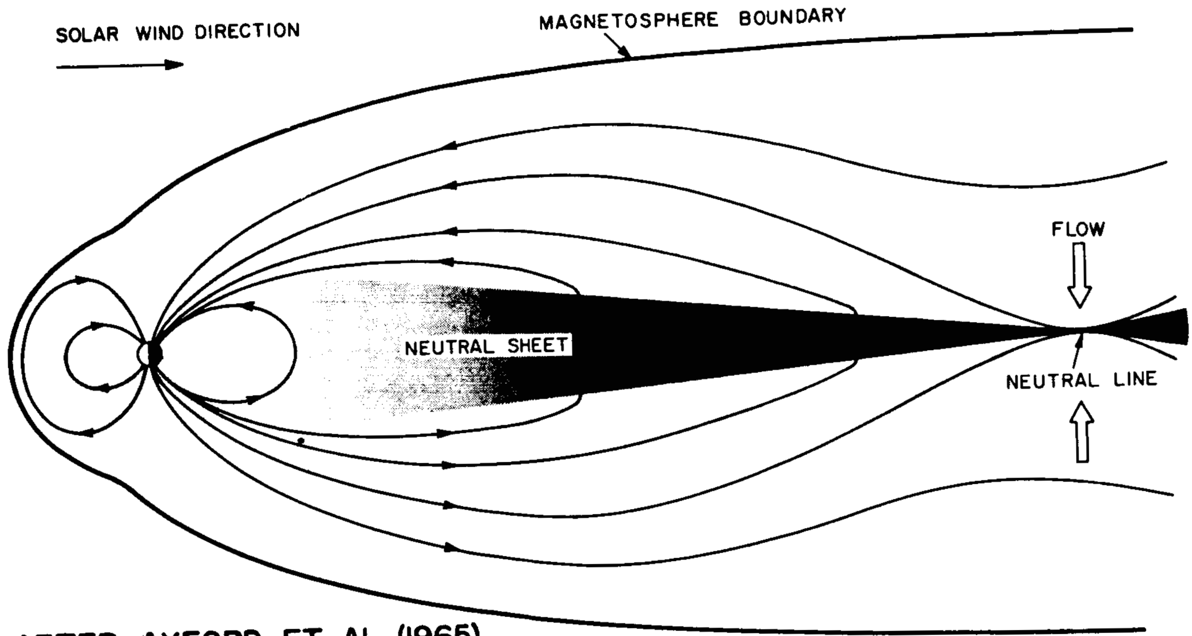

AFTER AXFORD ET. AL.(1965)

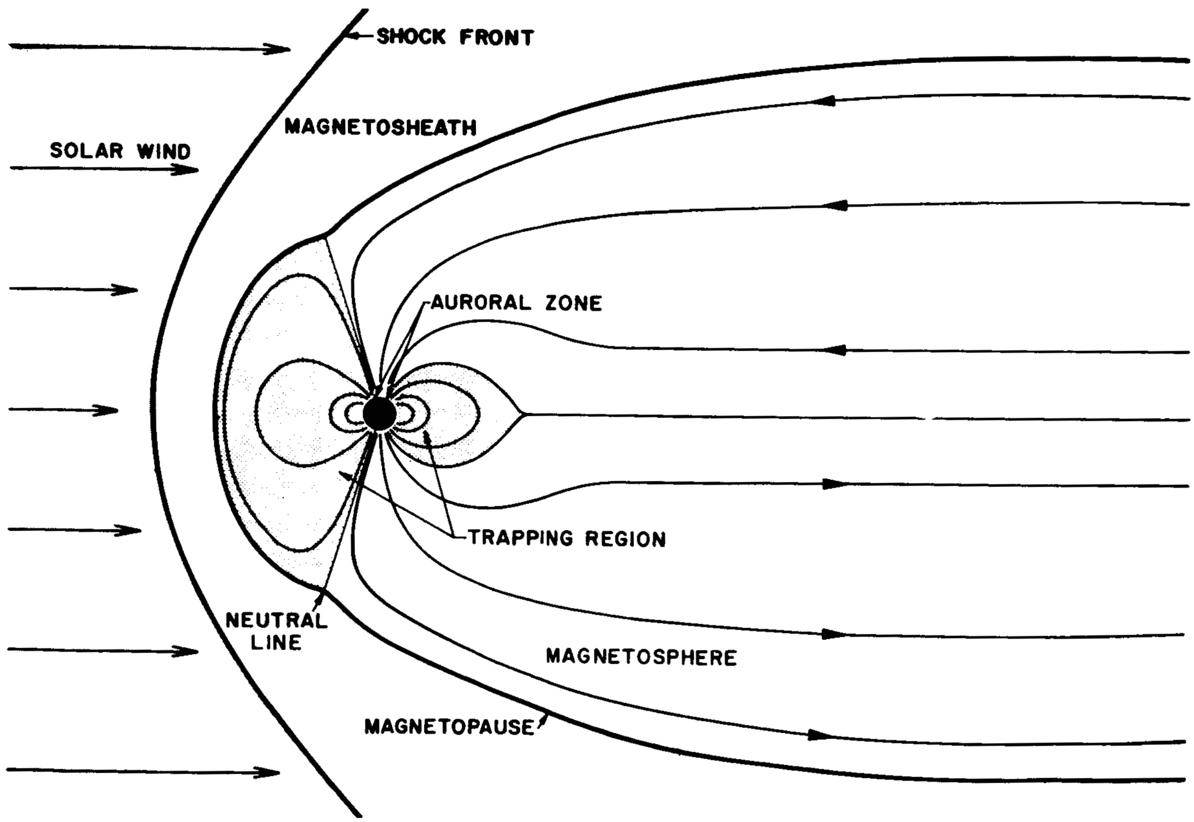

AFTER DESSLER & JUDAY (1965)

Figure 15

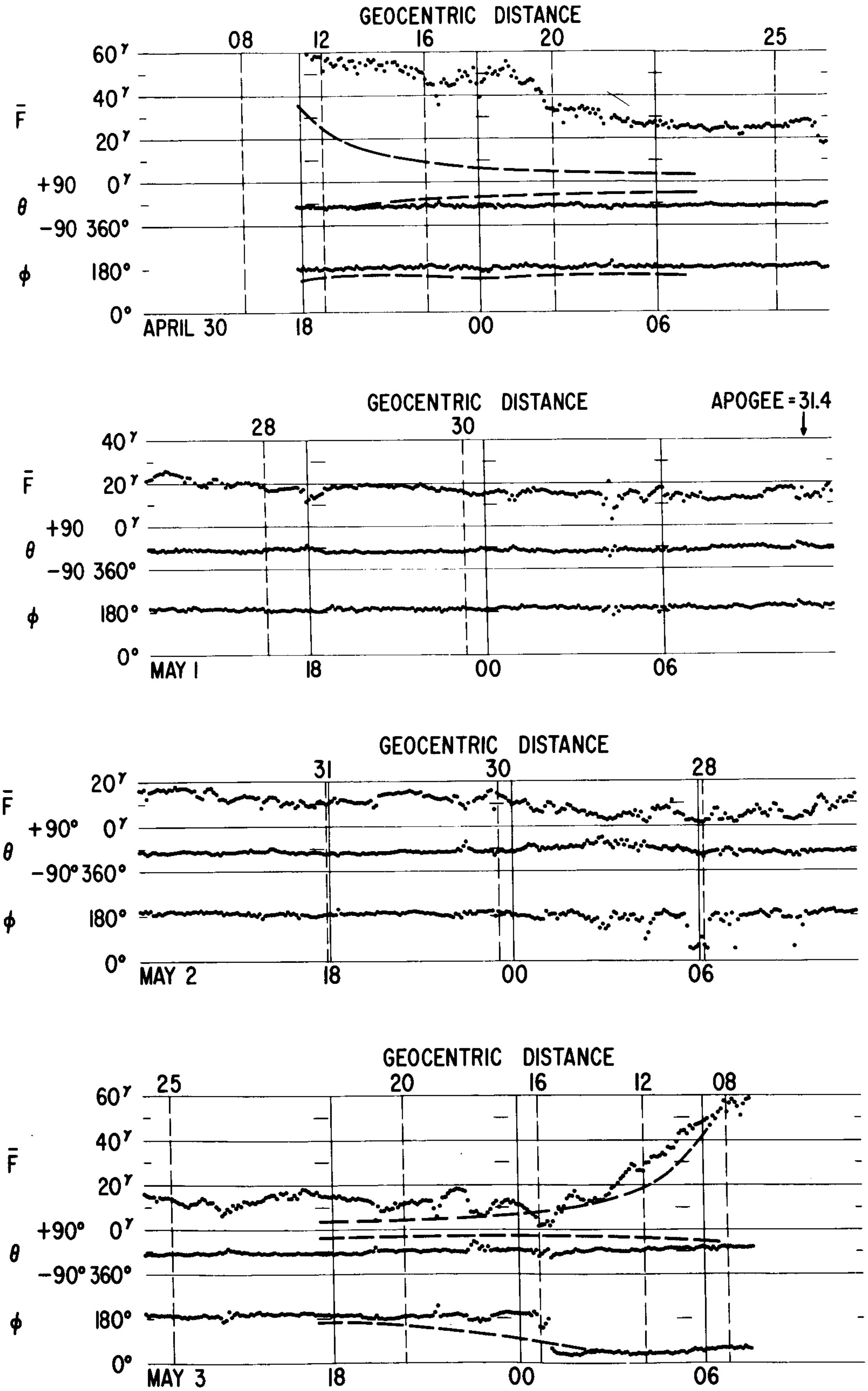

ORBIT NO. 41 IMP-1 1964

Figure 16

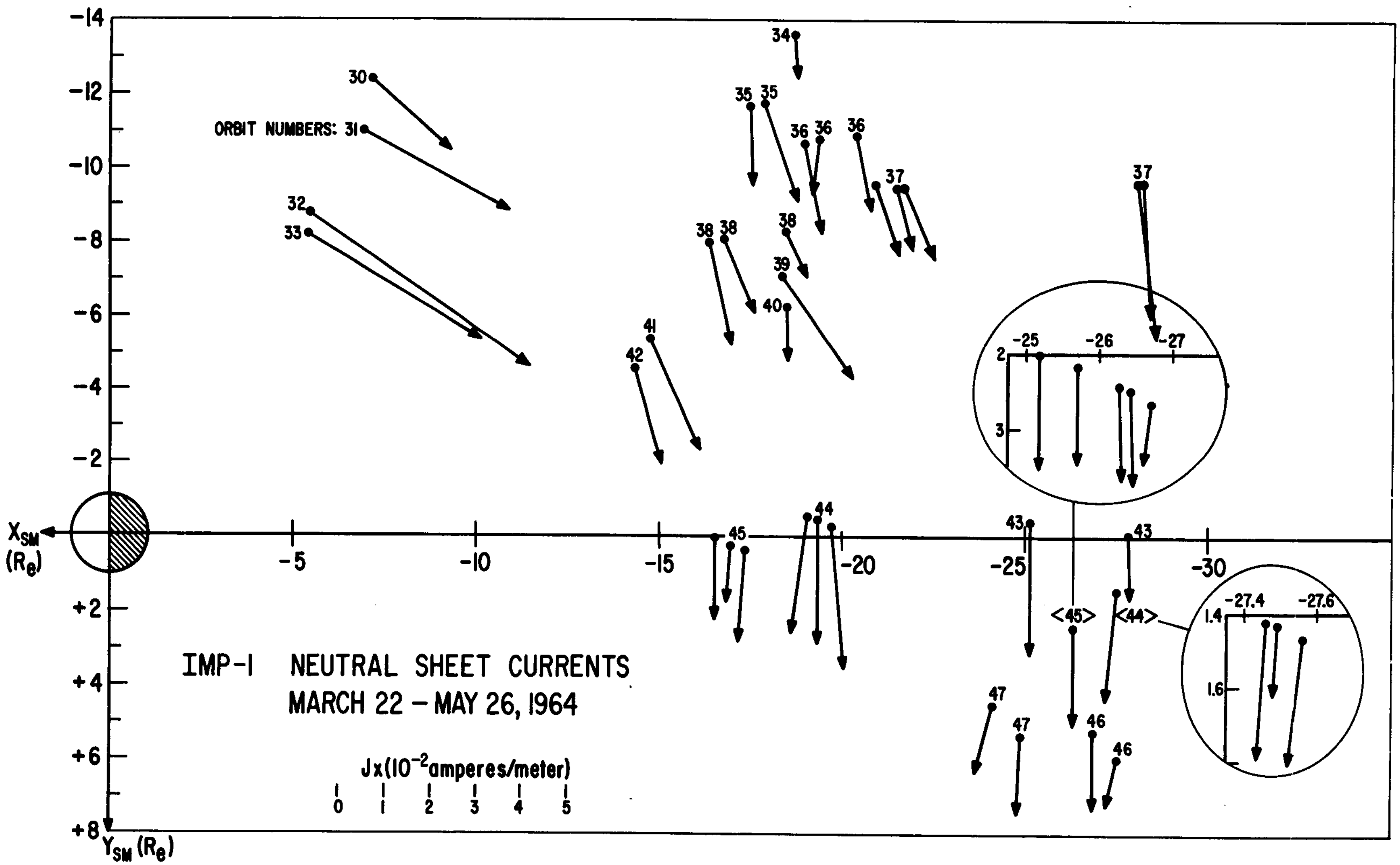
IMP-I NEUTRAL SHEET CURRENTS
MARCH 22 – MAY 26, 1964
Jx(10^-2 amperes/meter)
0 1 2 3 4 5
ORBIT NUMBERS: 31
30
32
33
34
35 35
36 36 36
37
37
38 38 38
39
40
41
42
43
43
44
45
<44>
<45>
46
46
47
47
X_SM (R_e)
Y_SM (R_e)
-14
-12
-10
-8
-6
-4
-2
+2
+4
+6
+8
-5
-10
-15
-20
-25
-30
-25
-26
-27
2
3
-27.4
-27.6
1.4
1.6

Figure 17

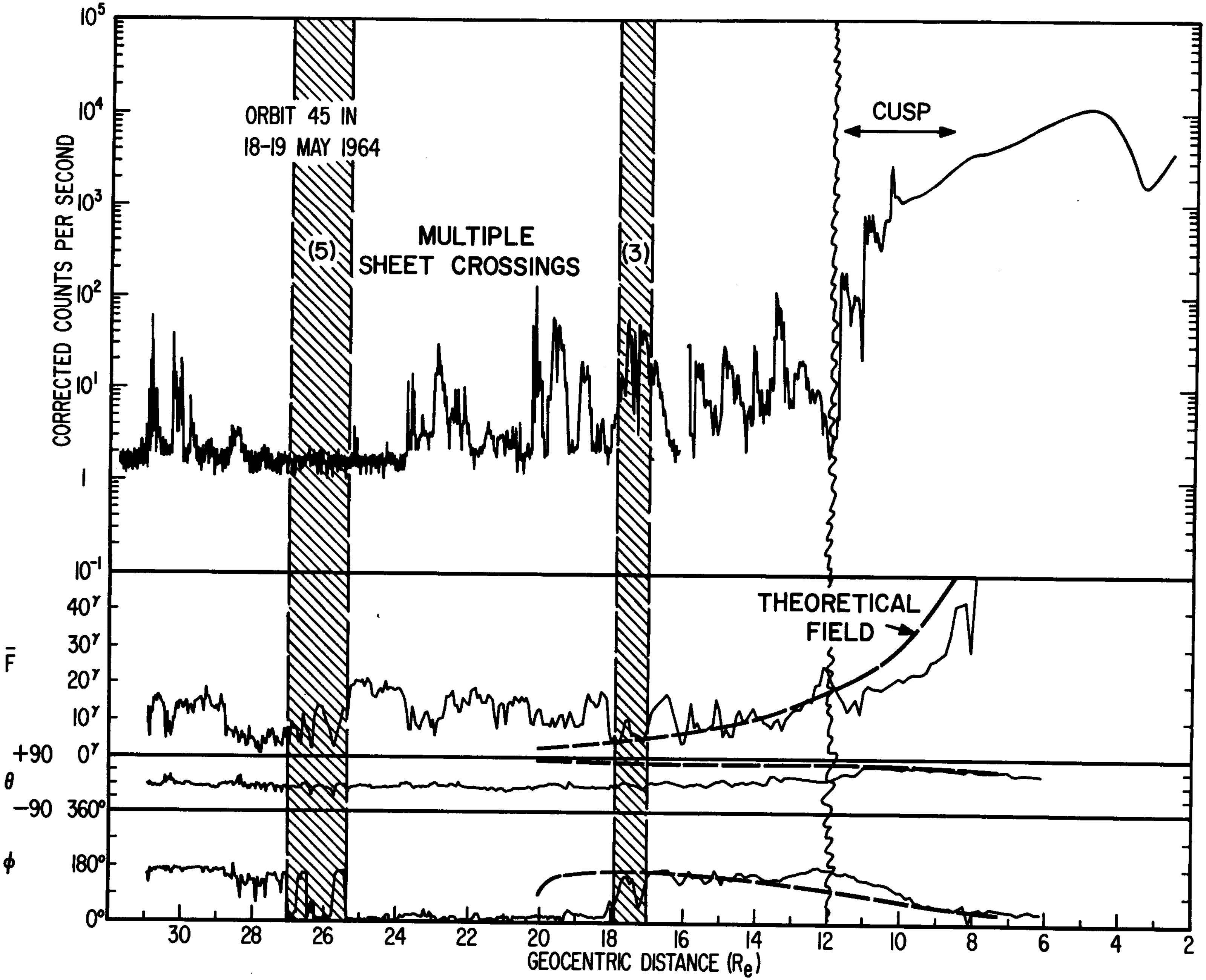
ORBIT 45 IN
18-19 MAY 1964
MULTIPLE
SHEET CROSSINGS
(5)
(3)
CUSP
THEORETICAL
FIELD
CORRECTED COUNTS PER SECOND
10^5
10^4
10^3
10^2
10^1
1
10^{-1}
40^γ
30^γ
20^γ
10^γ
0^γ
$\bar{F}$
+90
θ
−90
360°
180°
0°
ϕ
30
28
26
24
22
20
18
16
14
12
10
8
6
4
2
GEOCENTRIC DISTANCE (R_e)

Figure 18

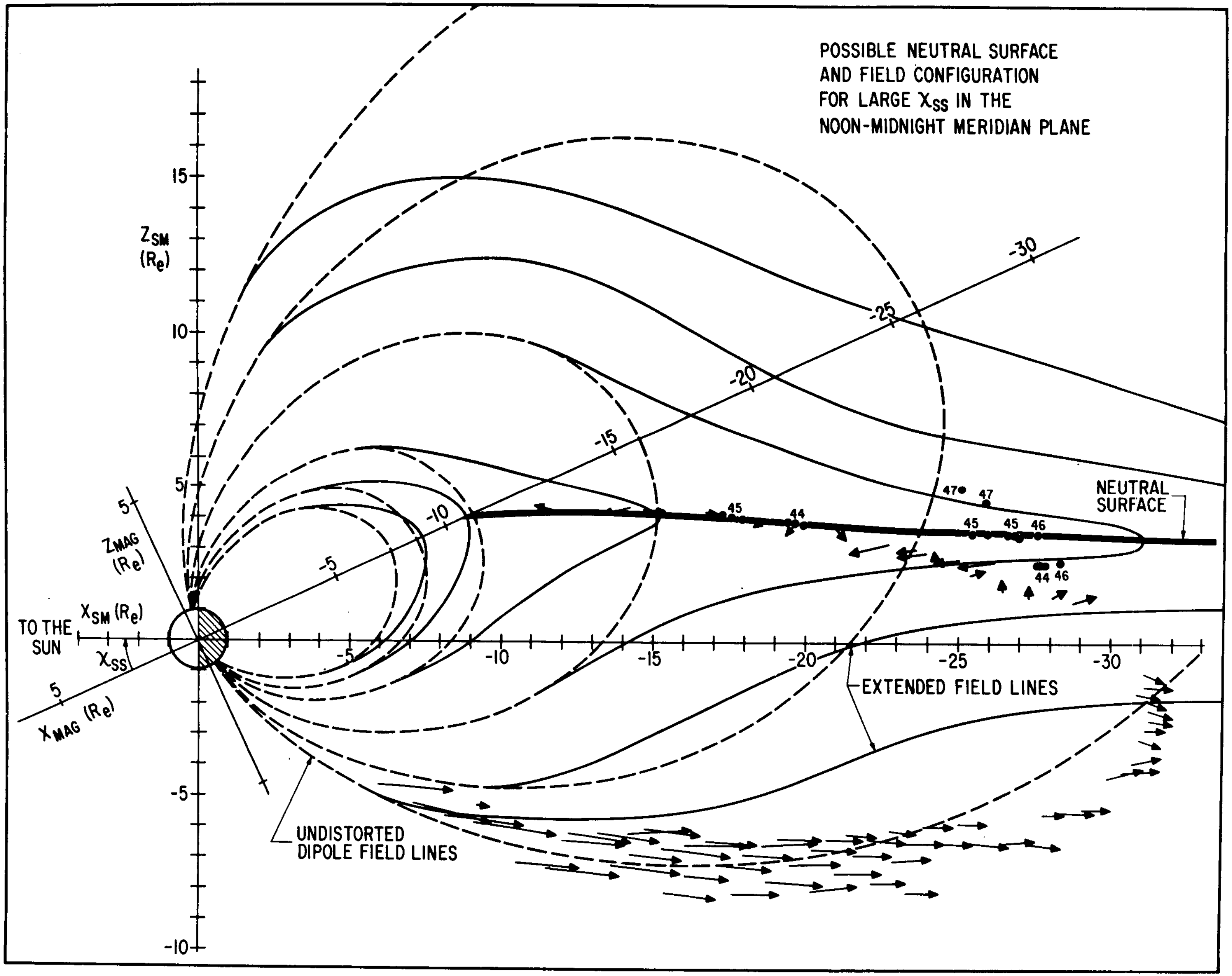
POSSIBLE NEUTRAL SURFACE
AND FIELD CONFIGURATION
FOR LARGE χ_{SS} IN THE
NOON-MIDNIGHT MERIDIAN PLANE
Z_{SM} (R_e)
Z_{MAG} (R_e)
X_{SM} (R_e)
X_{MAG} (R_e)
χ_{SS}
TO THE SUN
NEUTRAL SURFACE
EXTENDED FIELD LINES
UNDISTORTED DIPOLE FIELD LINES

Figure 19

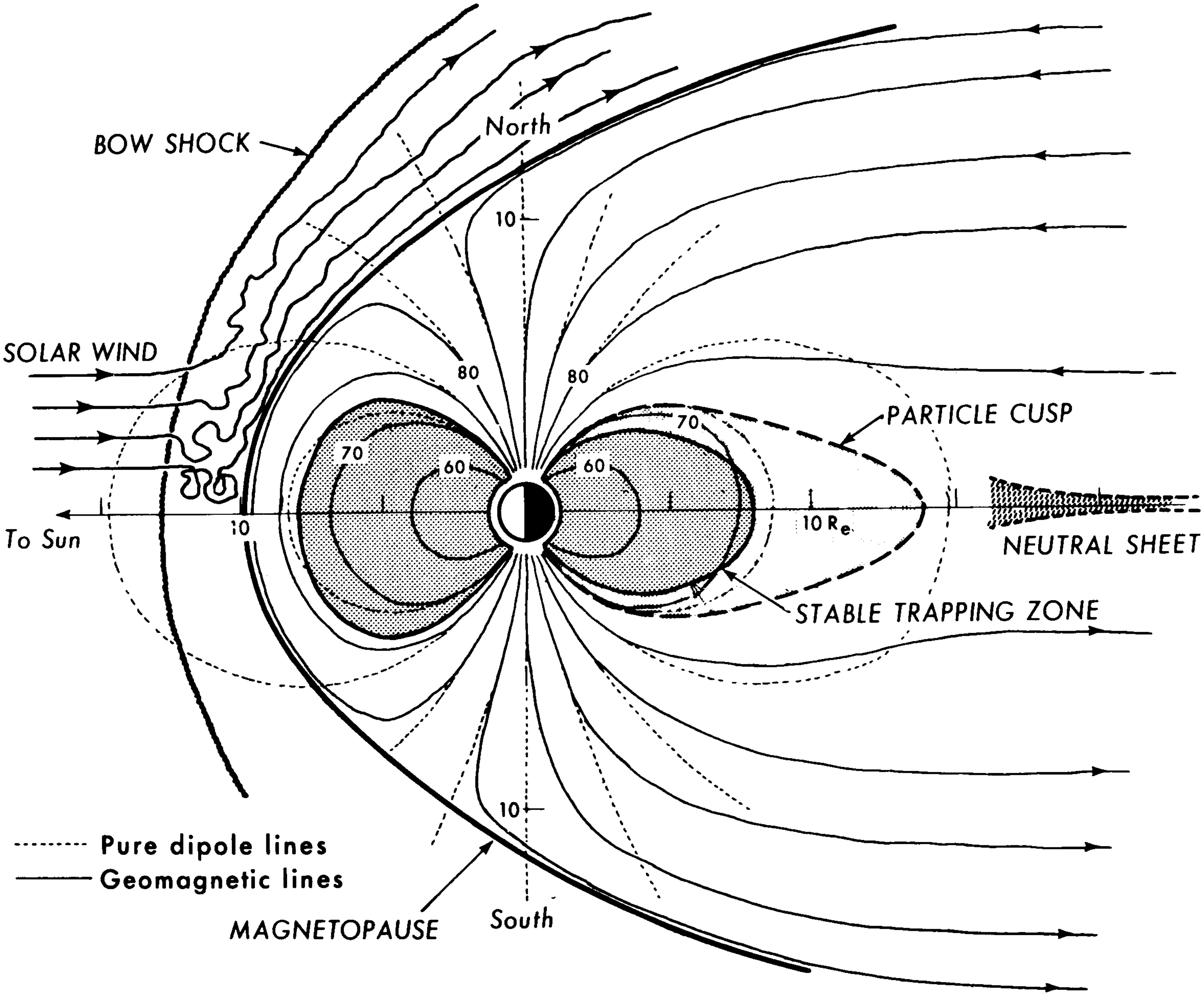
BOW SHOCK
North
SOLAR WIND
To Sun
10
80
80
70
70
60
60
10
10 R_e
PARTICLE CUSP
NEUTRAL SHEET
STABLE TRAPPING ZONE
10
Pure dipole lines
Geomagnetic lines
MAGNETOPAUSE
South

Figure 20